Doctoral Dissertation

Wireless light-emitting diode-driven functional microneedle devices for skin cancer therapy

MIRANDA OUNGEUN

Supervisor: Eijiro MIYAKO

Graduate School of Advanced Science and Technology
Japan Advanced Institute of Science and Technology
Materials Science

December 2024

Abstract

Photodynamic therapy, a non-invasive cancer treatment strategy, is one of the promising remedies for malignant skin cancers. This therapy provides many advantages; high accuracy, minimal invasiveness, availability of multiple irradiations at the same area, no long-term side effects, and high cost-performance. Treating skin cancer with this method, it is essential to permeate sufficient photosensitizer molecules into cancer cells before shining light for effective activation of photosensitizers in a tumor to express potent reactive oxygen species, such as superoxide (O_2^-), hydroxyl radical ($OH^\bullet$), singlet oxygen, and hydrogen peroxide (H_2O_2), for eradicating cancer cells. However, transdermal drug delivery using conventional photosensitizers has major challenges due to skin barriers, resulting in less effective drug penetration and therapeutic efficacies. To overcome these limitations, we applied biocompatible, physiologically dissolvable, and optically activatable functional microneedle devices for effective percutaneous penetration of drug molecules into the solid tumor under the skin of a mouse. One of the additional disadvantages of photodynamic therapy is the powerful laser light needed to activate the photosensitizer. After undergoing laser therapy, patients frequently experience skin burns, inflammation, edema, and redness due to the strong laser light energy. Herein, we considered wireless LED light-induced functional microneedle devices, effectively induce cancer cell apoptosis and disruption of the tumor area, could enhance *in vitro*, *ex vivo*, and *in vivo* drug delivery effectiveness for skin cancer treatment. The design and strategy of the present functional microneedle devices would help shed light on future advanced cancer therapy.

Keywords: skin cancer, dissolvable microneedles, light-emitting diode, photodynamic therapy, chemotherapy

Referee-in-chief: **Prof. Dr. Eijiro MIYAKO**

Japan Advanced Institute of Science and Technology

Referees: **Prof. Dr. Kazuaki MATSUMURA**

Japan Advanced Institute of Science and Technology, Japan

Prof. Dr. Motoichi KURISAWA

Japan Advanced Institute of Science and Technology, Japan

Prof. Dr. Takumi YAMAGUCHI

Japan Advanced Institute of Science and Technology, Japan

Prof. Dr. Supason WANICHWECHARUNGRUANG

Chulalongkorn University, Thailand

Table of contents

List of tables and figures

This dissertation was prepared according to the curriculum for the Collaborative Education Program organized by Japan Advanced Institute of Science and Technology and Chulalongkorn University.

CHAPTER 1

General introduction

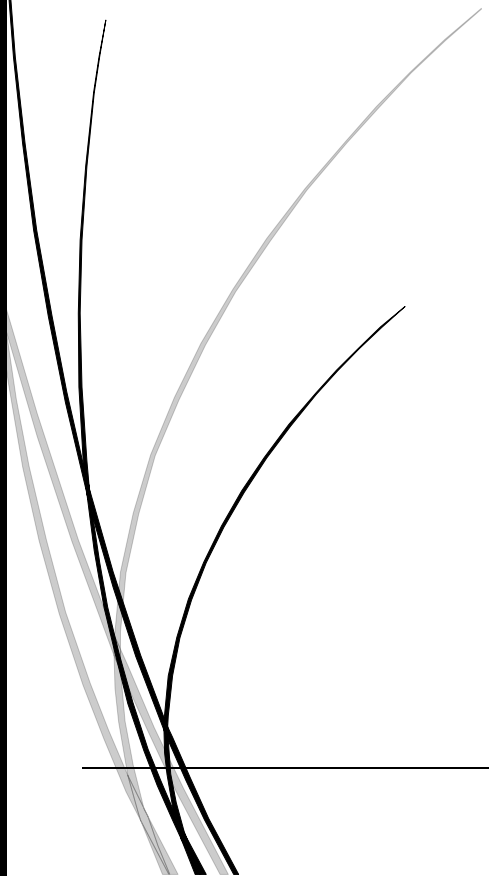

1.1 Introduction of skin cancer and treatments

The skin is the largest organ in the body. It accounts for approximately 15% of the body's weight.[1] The skin exfoliates and produces new skin cells continuously. Inappropriate division of the skin cell may cause it to spread and develop into skin cancer.[2] Skin cancer is found in approximately 5% of all cancers. It is often found among Caucasian people, people aged over 40 years, and in more men than women. There are three types of skin cancer: basal cell carcinoma, squamous cell carcinoma, and melanoma.[3-7]

Basal cell carcinoma (BCC) begins in the basal cells, which are cells that have a high ability to divide (mitotically active). The cell's shape is columnar with a large nucleus, found at the bottom of the epidermis. Basal cell carcinoma is the most common type of skin cancer. More than 80% of skin cancer patients have this type of skin cancer.[8] This type of carcinoma occurs when one of the skin's basal cells develops a mutation in its DNA. Basal cell carcinoma can arise from a variety of factors, including radiation therapy, aging, immunosuppressive medications, a personal or family history of skin cancer, and prolonged sun exposure. Prolonged sun exposure is thought to be the main cause of basal cell carcinoma.[8,9] Consequently, areas that are frequently exposed to sunlight are common areas to find this type of cancer, such as head and neck areas. It is found more in white people than in dark-skinned people.[10] Symptoms discovered include a smooth, shiny, pink, red, or skin-colored lump. There could be tiny capillaries visible on the bump's surface.[8,9]

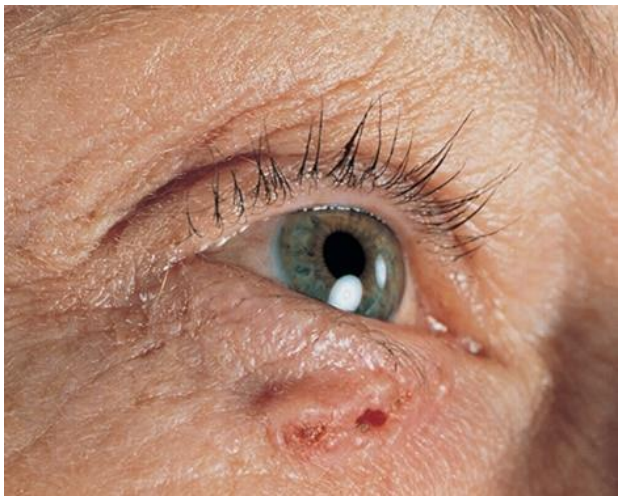

Figure 1.1 Basal cell carcinoma (BCC).[9]

Squamous cell carcinoma (SCC), or epidermoid carcinoma, is the second most common type of skin cancer. It often appears on areas of the skin that are exposed to sunlight as well. In white-skinned Westerners can be found in up to 20 percent of the total population.[11] Compared to basal cell carcinoma, squamous cell carcinoma can grow more quickly and has a larger chance of spreading to other parts of the body. The origin of squamous cell carcinoma is the squamous epithelial cell, a type of flat cell that is found in the middle layers of skin throughout the body, including the cervix, lips, and mouth. Squamous cell carcinoma can arise from a variety of factors, including immune deficiency, smoking, sunlight, toxins like arsenic, chronic wounds, radiation therapy, some wart viruses (such as the human papilloma virus), and hereditary abnormalities.[12,13] The symptoms include a raised bump with a hard base and a scaly top. It can also occasionally break into a wound, bleed, and enlarge.[14]

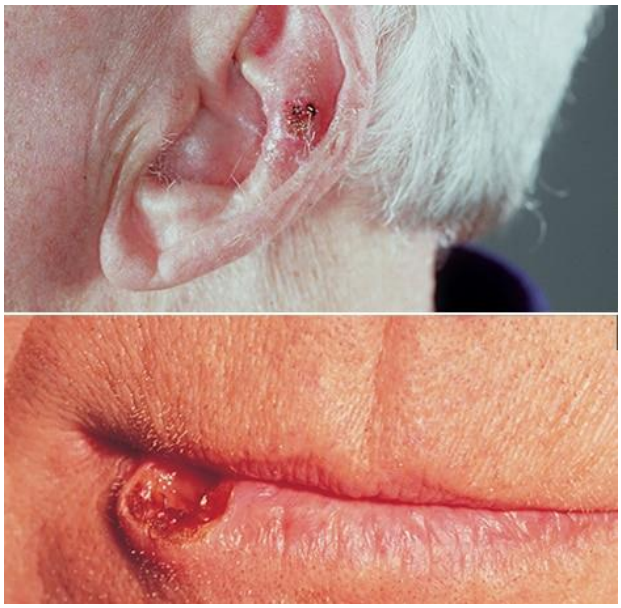

Figure 1.2 Squamous cell carcinoma (SCC).[14]

Basal cell carcinoma (BCC) and Squamous cell carcinoma (SCC) are the main types of non-melanoma skin cancer. The severity levels of non-melanoma skin cancer can be classified into 5 stages;[15,16]

• Stage 0 (Carcinoma in situ): A carcinoma indicates the presence of cancerous cells. The term "in situ" refers to the cells remaining where they began to develop. Thus, although the cells have begun to develop into cancer, they still have not proliferated or disseminated to neighboring skin regions.

• Stage I: Cancer has developed, and the tumor is no larger than 2 cm.

• Stage II: The tumor measures larger than 2 centimeters, but not larger than 4 centimeters.

• Stage III: The tumor measures larger than 4 centimeters. It spreads into the area surrounding a nerve (perineural invasion), beneath the subcutaneous tissue layer of fat beneath the skin, or close to bones. A tumor that is smaller than 4 centimeters but spreads to one lymph node on the same side of the body can be classified into this stage.

• Stage IV: Any size of cancer may have spread to the subcutaneous tissue or to the tissue surrounding the nerves beneath the dermis. It could damage bone by spreading to bone marrow or other bone, including the base of the skull. Additionally, there are already cancers in one or more lymph nodes.

Malignant melanoma is a cancer that arises from melanocytes that produce pigment in the skin. Compared to other types of skin cancer, this one is less frequent but more dangerous because it can quickly spread into the bloodstream. It is the cause of death for 75% of all skin cancer patients.[17] This kind of melanoma is usually observed in up to 160,000 cases worldwide annually, with the majority of cases occurring in the white population.[18] According to its characteristics, melanoma can be classified into five types: superficial spreading melanoma, nodular melanoma, lentigo maligna melanoma, acral lentiginous melanoma, and amelanotic melanoma. There are many causes of melanoma skin cancer. A significant factor is UV radiation exposure in sunlight. Additional causes include certain hereditary diseases, immune deficiency, chemicals such as arsenic, chronic wounds, radiation therapy, certain types of wart viruses (the human papilloma virus), smoking, etc.[19,20]

The severity levels of melanoma can be classified into 5 stages;[21,22]

• Stage 0 Melanoma (in situ): The malignant tumor is still limited to the epidermis, the topmost layer of the skin. It has not spread into the dermis, the second layer of skin. It has not spread beyond the primary tumor.

• Stage I Melanoma (localized tumor): Tumors can be found in both the epidermis and dermis. Melanoma is up to 2 mm thick and may or may not have ulceration. There is no evidence that the cancer has spread to lymph nodes or has metastasized.

• Stage II Melanoma (localized tumor): Tumor can be found in both the epidermis and dermis. The melanoma is more severe than Stage I. The tumor is deeper than stage I, and there is a presence of ulceration. The cancer has not spread to lymph nodes or has metastasized.

• Stage III Melanoma (regional spread): Tumor has spread to regional lymph nodes or has developed in-transit deposits of disease. However, no evidence of distant metastasis has been observed. It has reached the closest lymph nodes from the initial tumor, but it has not migrated to further areas.

• Stage IV Melanoma (metastasis beyond regional lymph nodes): Melanoma has spread beyond the initial tumor location and the local lymph nodes to more remote parts of the body. The most often metastasized sites for Stage IV melanoma, for example, bone, brain, lungs, liver, and/or intestines.

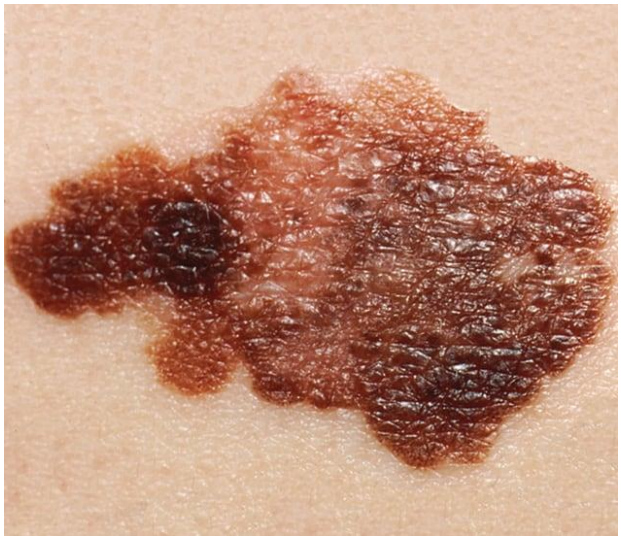

Figure 1.3 Malignant melanoma.[23]

There are currently a number of treatments available for skin cancer, such as surgery, curettage and electrodessication, cryotherapy, radiation therapy, chemotherapy, and photodynamic therapy.[24] The effectiveness of each cancer treatment method is different depending on the type of

skin cancer and the severity of the cancer. Dermatologists will use their discretion in choosing treatment methods that are appropriate for each patient. They can treat skin cancer more successfully by employing more than one therapy method.[25]

1.2 Standard cares of skin cancer

Skin cancer diagnosis is a prerequisite for treatment. The doctor may carry out the following examinations and procedures to identify skin cancer:[15,16,25-27]

• Skin exam: Checking the skin for lumps or areas that look abnormal in terms of size, color, form, or texture.

• Take a sample of skin that seems suspicious for testing (skin biopsy): The doctor may remove the suspicious-looking skin for lab testing. A biopsy can identify the type of skin cancer. The 4 principal types of skin biopsies are shave biopsy, punch biopsy, incisional biopsy, and excisional biopsy.

If patients are diagnosed with skin cancer, they may undergo further testing to ascertain the extent (stage) of the disease as follows:

• CT scan (CAT scan): A process that creates a number of detailed pictures of internal body parts, like the head, neck, and chest, from various perspectives. The images are created using a computer connected to an x-ray machine. The names for this process are computerized tomography, computerized axial tomography, and computed tomography.

• Chest x-ray: An x-ray is a kind of energy beam that can create an image of parts of the body by passing through it and onto film.

• Lymph node biopsy: The excision of a lymph node in its entirety or in part. A pathologist looks under a microscope at the tissue from the lymph nodes to check for cancerous cells.

• Positron emission tomography scan (PET scan): The process identifies cancerous cells within the body. A tiny quantity of sugar, or radioactive glucose, is injected into a vein. Since cancerous cells are more active and absorb more glucose than healthy cells, the PET scanner creates an image of the areas of the body where glucose is being consumed by cancerous cells and appears brighter in the image.

• Ultrasound exam: A process that creates echoes when high-energy sound waves, or ultrasonic waves, bounce off inside structures like lymph nodes or organs. The echoes create an image of body tissues called a sonogram. An ultrasonography examination of the local lymph nodes may be performed for basal cell carcinoma and squamous cell carcinoma of the skin.

Once patients have been informed of the type and stage of their skin cancer, a dermatologist will select the treatments that take into consideration the size, type, depth, location of the lesions, and stage of the skin cancer.

• Surgery: This type of treatment can be appropriate for any type of skin cancer. A dermatologist excises the malignant tissue and the surrounding margin of healthy skin.

• Cryosurgery: This technique, which uses liquid nitrogen to freeze cancerous tumors, can be appropriate for actinic keratoses and some early skin cancer. The dead tissue sloughs off when it thaws.

• Mohs micrographic surgery: The doctor removes the skin growth layer by layer until no abnormal cells are left under the microscope. This treatment is most appropriate for treating early-stage, localized skin cancers, particularly when the cancer is at stage 0 (carcinoma in situ) or stage I and stage II skin cancers. However, it may also be used in certain cases of higher-stage or recurrent cancers when precise removal is necessary.

• Radiation therapy: This treatment uses powerful energy beams, such as X-rays, to eliminate cancer cells. This treatment can be used for various stages of skin cancer. Its appropriateness depends on the type and specific circumstances of the cancer, including early-stage skin cancer (stages I and II), locally advanced skin cancer (stage III), and palliative treatment for advanced skin cancer (stage IV).

• Curettage and electrodesiccation: The tumor is cut from the skin with a curette, a sharp instrument created like a spoon. An electric current is then applied to the area using a needle-shaped electrode, which stops the bleeding and eliminates any cancer cells that might still exist around the wound's edge. This treatment is primarily appropriate for treating early-stage skin cancers, specifically stage 0 (carcinoma in situ) and stage I cancers. It is most often used for small, well-defined, superficial non-melanoma skin cancers due to its effectiveness in treating cancers that are not deeply invasive.

• Immunotherapy: This treatment against cancer through employing the patient's immune system. Immunotherapy is increasingly used for advanced-stage skin cancer, particularly for stage III and IV melanoma, and in certain cases for advanced squamous cell carcinoma (SCC). It is most beneficial for cancers that have spread beyond the primary site or that are resistant to traditional treatments.

• Chemotherapy: This treatment employs drugs that either kill or prevent the division of cancer cells to stop the growth of cancer cells. Chemotherapy is typically used for advanced-stage skin cancer (usually stage III or IV) or for cases where other treatments, like surgery or radiation, are not effective or possible. It is generally not the first-line treatment for most types of skin cancer, particularly non-melanoma skin cancers like basal cell carcinoma (BCC) and squamous cell carcinoma (SCC), which are often treated with localized therapies.

• Photodynamic therapy: Photodynamic therapy is a cancer treatment that eliminates cancer cells by combining a drug with a certain kind of light. The drug, which is either applied or injected into a vein, accumulates higher in cancer cells than in normal cells. A drug is inactive until it is exposed to light. Photodynamic therapy is primarily used for early-stage, superficial skin cancers, particularly stage 0 (carcinoma in situ) and stage I cancers. PDT is most effective for non-melanoma skin cancers that are located on or near the surface of the skin, as well as for some precancerous lesions.

1.3 Photodynamic therapy

Photodynamic therapy is one of the most widely used methods for treating cancer. This method is frequently used to treat many types of cancer, such as pancreatic cancer, bile duct cancer, esophageal cancer, lung cancer, brain cancer, and is commonly used to treat certain skin diseases (actinic keratosis and nonmelanoma skin cancer).[28] To treat skin cancer using photodynamic therapy, dermatologists first exfoliate the skin to eliminate dry skin or crusting before applying a photosensitizer (PS) and waiting at least three hours for the agent to penetrate the cancer cells. Then, involving the doctor shining light on the skin to activate photosensitizer to generate reactive oxygen species (ROS), including superoxide (O_2^-), hydroxyl radical ($OH^\bullet$), singlet oxygen, and hydrogen peroxide (H_2O_2), to kill cancer cells.[29] Photodynamic therapy has several benefits for the treatment of cancer, including high precision, less invasiveness than surgery, repeatability in the same location, lack of long-term side effects, and lower cost compared to other skin cancer treatments.[30] However, the limitations of photodynamic therapy still exist. Since applying drugs to the cancer tumor is the strategy used in photodynamic therapy, this can cause limitations in drug delivery efficiency due to the stratum corneum (outer layer of the skin), which functions as a barrier to prohibit foreign objects from entering the body through the skin.[31] As a result, the applied

drug is unable to be delivered to the cancerous tumor as effectively, which affects the efficiency of treating skin cancer. Moreover, adverse effects from photodynamic therapy still result from the use of high-intensity laser light to stimulate the photosensitizer's activity. After undergoing laser therapy, patients frequently report experiencing skin burns, inflammation, edema, and redness.[32,33]

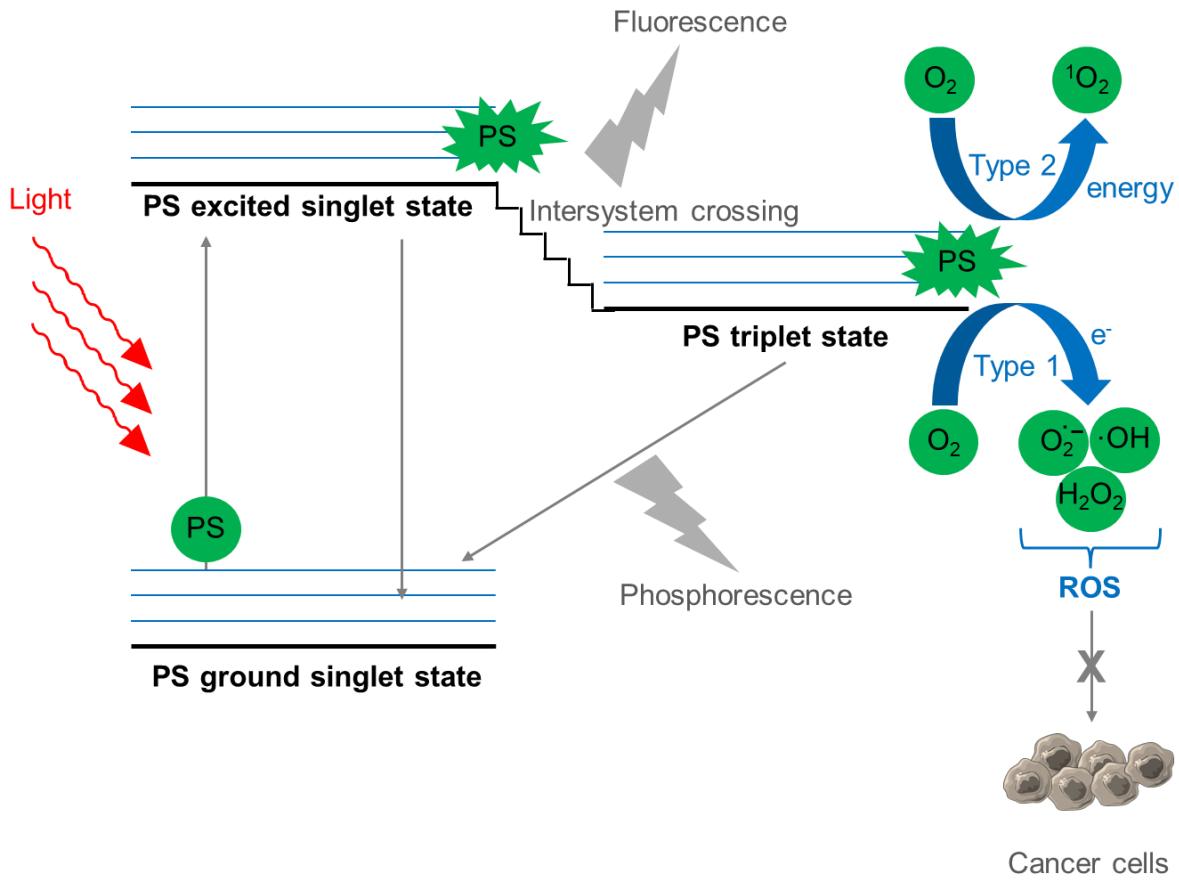

Figure 1.4 Schematic illustration of photodynamic therapy.[29]

1.4 Dissolvable microneedles

Microneedles (MN) are micron-sized needles, ranging from 25 to 2000 μm in height, made of a variety of materials and shapes.[34] Application of MNs to the skin can create micron-sized transport pathways that allow enhanced delivery of a wide range of drug molecules. MNs were first

introduced in 1971 by Gerstel and V. A. Place, which were made from silicon. The initial concept was to create skin micropores before applying drugs.[35,36] With the advancement of technology, there are now five main categories of microneedle technology: solid, coated, hollow, hydrogel-forming, and dissolvable.[36] Dissolvable microneedles (DMNs) are one of the MNs used to enhance drug delivery through the skin. They were first published in the report in 2005 by Miyano et al. They created DMNs from maltose, a disaccharide made from two units of glucose, to distribute vitamin C through the skin.[34] DMNs can be formed by several methods, including droplet air blowing[37], drawing lithography[38], photopolymerization[38], and micromolding[38]. Currently, it can be molded from a variety of materials that must have properties such as being harmless, degradable in human skin, cellularly compatible, and biocompatible.[39,40] These materials are commonly used in the molding of DMNs, for example, gelatin[41,42], polyvinyl alcohol (PVA)[43], polyvinylpyrrolidone (PVP)[44], hyaluronic acid (HA)[45], and sugars[46,47]. The working principle of DMNs is that when they are implanted into the skin, the needle will dissolve in the interstitial fluid in the skin and release the loaded drug into the skin. The advantages of using DMNs for transdermal drug delivery are that they are drug release-controlled, safe, non-invasive, inexpensive, self-administered, non-biohazardous, and waste-sharpless.[39] DMNs have reportedly been used to deliver different active compounds into the skin. Among them is the delivery of cancer drugs. For example, in the study by Ye et al.[48] They used hyaluronic acid (HA)-based microneedles to deliver the immunoinhibitory receptor programmed cell death protein 1 (PD1) and the immunosuppressive enzyme indoleamine 2,3-dioxygenase (IDO) to B16F10 melanoma in immunotherapy. The results demonstrated that HA-DMNs sustained the release and enhanced retention of checkpoint inhibitors in the tumor microenvironment. Furthermore, it was shown that combining PD1 with IDO produced a synergistic effect that improved the effectiveness of cancer

treatment. In the study by Fu et al.,[49] they used dissolvable microneedles fabricated from vinylpyrrolidone-vinyl acetate copolymer (PVPVA) to deliver two types of cancer drugs: photosensitizer IR820 and chemotherapy agent cisplatin (CDDP) for chemo-photodynamic therapy against breast cancer. The results demonstrated that PVPVA-DMNs performed well at delivering drugs to the skin. The needle dissolved within 10 minutes after being inserted into murine skin. Furthermore, it was discovered that the combination of IR820 (photosensitizer) with CDDP (chemotherapy drug) results in a more effective synergistic effect on cancer eradication than either drug used alone.

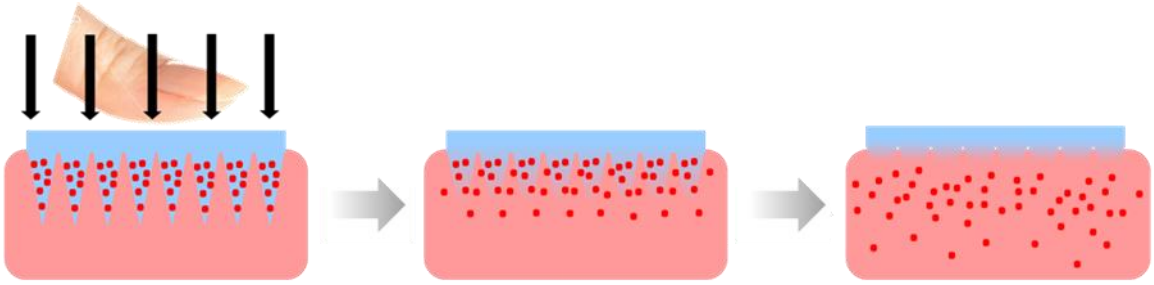

Figure 1.5 Dissolution mechanism of dissolvable microneedles.

1.5 Light-emitting diode

LED is a semiconductor device that combines a P-type region (positive charges, larger hole concentration). P-type regions are typically made of elements or compounds that have free-valence electrons, typically silicon (Si) or germanium (Ge).[50] Another part is the N-type region (negative charges, larger electron concentration). N-type regions are typically made of elements or compounds that have extra-valence electrons, typically phosphorus (P), arsenic (As), or antimony (Sb).[51] An LED operates on the basis that when it receives a sufficient voltage, current flows and electrons move across the junction from the N region into the P region, where the negatively charged electrons combine with positive charges. Each combination of charges is associated with

an energy level reduction that may release a quantum of electromagnetic energy in the form of a light photon.[52] Making changes in the characteristics of the semiconductor material allows for the various frequencies and perceived colors of emitted photons.

The origin of LED lighting begins with the discovery of electroluminescence. The creation of LED lights is based on the electroluminescence principle.[55] This occurrence was observed in 1907 by Henry Joseph Round of Marconi Laboratories using a silicon carbide crystal and a cat's-whisker detector.[56] The first light-emitting diode for practical application was created in the 1950s using semiconductor gallium arsenide. The development of LEDs continued until 1962, when Nick Holonyak, Jr. created the first LED that produced red light that could be clearly observed while working for General Electric.[57] With the advantages of LED are that its long-lasting capability, low power requirements, swift response time, and fast switching capabilities.[54] Nowadays, there are many types of LEDs that have been invented, including miniature LEDs, high-power LEDs, flash LEDs, bi- and tri-color LEDs, alphabetic LEDs, and lighting LEDs.[53] LEDs have been developed and employed in a wide range of applications including robotics, optical communication, remote control operations, security and alarm systems, and, especially recently, photodynamic therapy for the treatment of cancer.[58-60] For example, Shi et al.[59] investigated the application of three different LED types: intense, sparse, and point, to increase the activity of hematoporphyrin derivatives (photosensitizers) in the eradication of gastrointestinal cancer in both *in vitro* and *in vivo* experiment. The experimental results demonstrated that the type of LED array significantly affected the performance of PDT for gastrointestinal cancer. Intensive LED-PDT induced earlier and more serious cell death, including apoptosis and necrosis, than sparse LED-PDT and point LED-PDT. Choi et al.[60] investigated the use of an implantable micro-scale LED by implanting the LED into the core of a tumor to generate mild visible light and activate the

verteporfn (photosensitizer) in order to eradicate CT26 colon tumors in mice. The results demonstrated that 100% total tumor regression can be achieved with implanted micro-LED guided PDT in combination with immune checkpoint suppression. Furthermore, the procedure creates systemic immunological memory that helps prevent tumor recurrence.

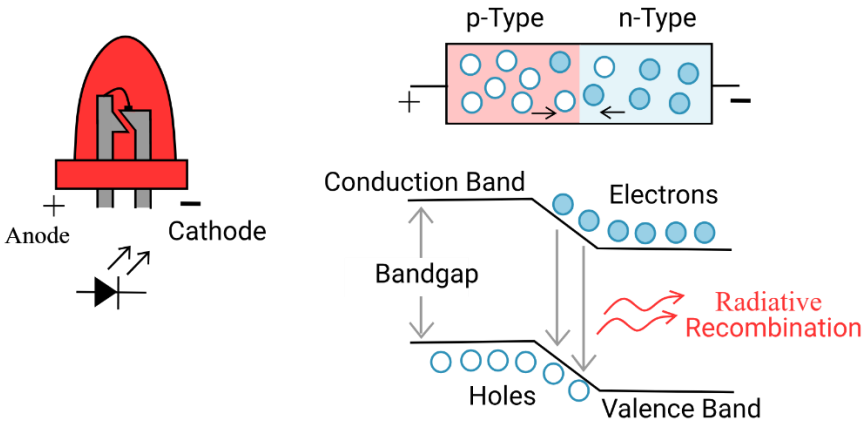

Figure 1.6 The principal operation of LEDs.[61]

1.6 Purpose and outlines

Dissolvable microneedles (DMNs) are an effective device for delivering drugs into the skin with the ability to regulate drug release rate, safety, non-invasiveness for the user, cost-effectiveness, and lack of sharp waste. Numerous studies have reported on the use of DMNs to deliver various types of active compounds. One such application involves the delivery of photosensitizer into the skin before light-shining to treat cancer following a photodynamic procedure. The results demonstrated that DMNs help deliver drugs into the skin more efficiently, resulting in improved cancer treatment efficiency. Moreover, the use of a high-intensity laser for stimulating photosensitizer was also considered due to reports that patients experienced skin burns, inflammation, edema, and redness after light shining. Shining light from LEDs instead of using

high-intensity laser light to stimulate the photosensitizer is an interesting method as an alternative light source for treating skin cancer using photodynamic techniques.

Based on the previously provided information, the researcher created the microneedle optical device (MOD), a device for skin cancer treatment employing photodynamic therapy strategies. The device consists of two parts. One is a part of dissolvable microneedles (DMNs) fabricated from sorbitol in micron-sized needles containing chlorin e6, a photosensitizer, and doxorubicin, a chemotherapeutic drug. When these two drugs are used in combination, they provide a synergistic effect that improves the result of skin cancer treatment. Another part is a small light-emitting bulb. The researchers used LEDs instead of high-intensity laser light. Using LED causes fewer negative effects and is less expensive than using laser light. The usage of MOD is in two steps, the first step is to puncture the DMNs loading drugs onto the skin tumor area. The sorbitol needle dissolves in the interstitial fluid of the skin, allowing the drugs to be released into the skin. The support will be peeled off then. The second step involves applying the LED to the skin to activate chlorin e6's activity. The goal of the research is to develop a novel approach to treat skin cancer with this microneedle optical device (MOD). We would like to create a device that effectively combats skin cancer while minimizing the adverse effects from employing high-intensity lasers. Without the use of laser equipment, the MOD is smaller in size, which is easier to use, has a lower price, and can be developed as a self-use device following the dermatologist’s guidance. The self-use feature of this device and its reasonable price make it appropriate for people who cannot afford hospital medical care or who live far from a medical facility. This device may be utilized to suppress the growth of cancerous tumors in patients before receiving further treatment.

1.7 References

(1) Richardson, M. Understanding the Structure and Function of the Skin. *Nurs. Times* **2003**, *99* (31), 46–48.

(2) *What are basal and squamous cell skin cancers.* Cancer.org. https://www.cancer.org/cancer/types/basal-and-squamous-cell-skin-cancer/about/what-is-basal-and-squamous-cell.html (accessed 2024-04-30).

(3) *Childhood melanoma treatment (PDQ®).* National Cancer Institute. https://www.cancer.gov/types/skin/hp/child-melanoma-treatment-pdq (accessed 2024-03-20).

(4) Leiter, U.; Eigentler, T.; Garbe, C. Epidemiology of Skin Cancer. In Sunlight, Vitamin D and Skin Cancer; Springer New York: New York, NY, **2014**; pp 120–140.

(5) *Types of skin cancer.* American Academy of Dermatology Association. https://www.aad.org/public/diseases/skin-cancer/types/common (accessed 2024-04-30).

(6) Shao, K.; Feng, H. Racial and Ethnic Healthcare Disparities in Skin Cancer in the United States: A Review of Existing Inequities, Contributing Factors, and Potential Solutions. *J. Clin. Aesthet. Dermatol*. **2022**, *15* (7), 16–22.

(7) *Melanoma skin cancer.* Cedars-Sinai. https://www.cedars-sinai.org/health-library/diseases-and-conditions/m/melanoma-skin-cancer.html (accessed 2024-04-30).

(8) Chung, S. Basal Cell Carcinoma. *Arch. Plast. Surg.* **2012**, *39* (02), 166–170.

(9) *Basal cell carcinoma.* Mayo Clinic. https://www.mayoclinic.org/diseases-conditions/basal-cell-carcinoma/symptoms-causes/syc-20354187 (accessed 2024-04-30).

(10) *Basal cell carcinoma in skin of colour.* Dermnetnz.org. https://dermnetnz.org/topics/basal-cell-carcinoma-in-skin-of-colour (accessed 2024-04-30).

(11) Nanz, L.; Keim, U.; Katalinic, A.; Meyer, T.; Garbe, C.; Leiter, U. Epidemiology of Keratinocyte Skin Cancer with a Focus on Cutaneous Squamous Cell Carcinoma. *Cancers (Basel)* **2024**, *16* (3), 606.

(12) Cohen, P. R.; Erickson, C. P.; Calame, A. Cutaneous Squamous Cell Carcinoma Masquerading as a Verruca: Case Report and Literature Review of Coexisting Wart and Invasive Squamous Cell Carcinoma on the Hand. *Cureus* **2022**.

(13) *Basal and squamous cell skin cancer risk factors.* Cancer.org. https://www.cancer.org/cancer/types/basal-and-squamous-cell-skin-cancer/causes-risks-prevention/risk-factors.html (accessed 2024-04-30).

(14) *Squamous cell carcinoma of the skin.* Mayo Clinic. https://www.mayoclinic.org/diseases-conditions/squamous-cell-carcinoma/symptoms-causes/syc-20352480 (accessed 2024-04-30).

(15) *National cancer institute (.Gov). Cancer.gov.* https://www.cancer.gov/types/skin/patient/skin-treatment-pdq (accessed 2024-11-14).

(16) *Stages and grades of skin cancer*. (n.d.). Cancerresearchuk.org. https://www.cancerresearchuk.org/about-cancer/skin-cancer/stages-grades (accessed 2024-11-14).

(17) Sirvan, S. S. Approach to Patients with Malignant Melanoma of Unknown Primary Origin. SiSli Etfal Hastan. *Tip Bul. / Med. Bull. Sisli Hosp*. **2019**.

(18) Zhang, K. S.; Pelleg, T.; Campbell, S.; Rubio, C.; Loschner, A. L.; Ie, S. Pulmonary Metastatic Melanoma: Current State of Diagnostic Imaging and Treatments. *Melanoma Manag*. **2021**, *8* (3).

(19) *Melanoma skin cancer risk factors.* Cancer.org. https://www.cancer.org/cancer/types/melanoma-skin-cancer/causes-risks-prevention/risk-factors.html (accessed 2024-04-30).

(20) *What causes melanoma.* Cancer.org. https://www.cancer.org/cancer/types/melanoma-skin-cancer/causes-risks-prevention/what-causes.html (accessed 2024-04-30).

(21) *Treatment of melanoma by stage*. (n.d.). Cancer.org. https://www.cancer.org/cancer/types/melanoma-skin-cancer/treating/by-stage.html (accessed 2024-11-14).

(22) *Stages of melanoma*. (2019, June 10). AIM at Melanoma Foundation. https://www.aimatmelanoma.org/stages-of-melanoma/ (accessed 2024-11-14).

(23) *Melanoma*. Mayo Clinic. https://www.mayoclinic.org/diseases-conditions/melanoma/symptoms-causes/syc-20374884 (accessed 2024-04-30).

(24) *Understanding Skin Cancer*; Mothoneos, J., Eds.; Cancer Council, Level 14, 477 Pitt Street, Sydney, Australia **2020**.

(25) *Skin cancer.* Mydermatologyassociates.com. https://www.mydermatologyassociates.com/skin-cancer-treatment/ (accessed 2024-04-30).

(25) *Skin cancer*. (n.d.). Mayoclinic.org. Retrieved November 14, 2024, from https://www.mayoclinic.org/diseases-conditions/skin-cancer/diagnosis-treatment/drc-20377608

(26) *Skin cancer*. (n.d.-b). Cleveland Clinic. Retrieved November 14, 2024, from https://my.clevelandclinic.org/health/diseases/15818-skin-cancer

(27) Hasan, N.; Nadaf, A.; Imran, M.; Jiba, U.; Sheikh, A.; Almalki, W. H.; Almujri, S. S.; Mohammed, Y. H.; Kesharwani, P.; Ahmad, F. J. Skin cancer: understanding the journey of transformation from conventional to advanced treatment approaches. *Molecular Cancer*. **2023**, *22* (1), 168.

(28) Gunaydin, G.; Gedik, M. E.; Ayan, S. Photodynamic Therapy for the Treatment and Diagnosis of Cancer–A Review of the Current Clinical Status. *Front. Chem.* **2021**, *9*.

(29) Kessel, D. Photodynamic Therapy: A Brief History. *J. Clin. Med.* **2019**, *8* (10), 1581.

(30) *PDT*. Cancer.org. https://www.cancer.org/cancer/managing-cancer/treatment-types/radiation/photodynamic-therapy.html (accessed 2024-04-30).

(31) Alkilani, A.; McCrudden, M. T.; Donnelly, R. Transdermal Drug Delivery: Innovative Pharmaceutical Developments Based on Disruption of the Barrier Properties of the Stratum Corneum. *Pharmaceutics* **2015**, *7* (4), 438–470.

(32) Bryce, R. Burns after Photodynamic Therapy. *BMJ* **2000**, *320* (7251), 1731–1731.

(33) *Photodynamic therapy to treat cancer.* Cancer.gov. https://www.cancer.gov/about-cancer/treatment/types/photodynamic-therapy (accessed 2024-04-30).

(34) Aldawood, F. K.; Andar, A.; Desai, S. A Comprehensive Review of Microneedles: Types, Materials, Processes, Characterizations and Applications. *Polymers (Basel)* **2021**, *13* (16), 2815.

(35) He, X.; Sun, J.; Zhuang, J.; Xu, H.; Liu, Y.; Wu, D. Microneedle System for Transdermal Drug and Vaccine Delivery: Devices, Safety, and Prospects. *Dose Response* **2019**, *17* (4), 155932581987858.

(36) Rzhevskiy, A. S.; Singh, T. R. R.; Donnelly, R. F.; Anissimov, Y. G. Microneedles as the Technique of Drug Delivery Enhancement in Diverse Organs and Tissues. *J. Control. Release* **2018**, *270*, 184–202.

(37) Kim, J. D.; Kim, M.; Yang, H.; Lee, K.; Jung, H. Droplet-Born Air Blowing: Novel Dissolving Microneedle Fabrication. *J. Control. Release* **2013**, *170* (3), 430–436.

(38) Hao, Y.; Li, W.; Zhou, X.; Yang, F.; Qian, Z. Microneedles-Based Transdermal Drug Delivery Systems: A Review. *J. Biomed. Nanotechnol.* **2017**, *13* (12), 1581–1597.

(39) Ita, K. Dissolving Microneedles for Transdermal Drug Delivery: Advances and Challenges. *Biomed. Pharmacother.* **2017**, *93*, 1116–1127.

(40) Nguyen, H. X.; Nguyen, C. N. Microneedle-Mediated Transdermal Delivery of Biopharmaceuticals. *Pharmaceutics* **2023**, *15* (1), 277.

(41) Ryota, N.; Hirofumi, M.; Shigeki, T. A Novel Microneedle Device Having Flexible Substrate and Strong Needles Using PVA and Gelatin. *2017 International Symposium on Micro-NanoMechatronics and Human Science (MHS)*; IEEE, 2017.

(42) Chiu, T.-M.; Hsu, P.-C.; Khan, M. Y.; Lin, C.-A. J.; Lee, C.-H.; Hsu, T.-C.; Chen, M.-H.; Hanagata, N. A Perspective on Imiquimod Microneedles for Treating Warts. *Pharmaceutics* **2021**, *13* (5), 607.

(43) Terashima, S.; Tatsukawa, C.; Suzuki, M.; Takahashi, T.; Aoyagi, S. Twice Stretched Fabrication of Polylactic Acid Microneedle Arrays Using Drawing Lithography. *Int. J. Precis. Eng. Manuf.* **2020**, *21* (10), 1933–1942.

(44) Lee, C.; Kim, J.; Um, D. J.; Kim, Y.; Min, H. S.; Shin, J.; Nam, J. H.; Kang, G.; Jang, M.; Yang, H.; Jung, H. Optimization of Layered Dissolving Microneedle for Sustained Drug Delivery Using Heat-Melted Poly(Lactic-Co-Glycolic Acid). *Pharmaceutics* **2021**, *13* (7), 1058.

(45) Fakhraei Lahiji, S.; Kim, Y.; Kang, G.; Kim, S.; Lee, S.; Jung, H. Tissue Interlocking Dissolving Microneedles for Accurate and Efficient Transdermal Delivery of Biomolecules. *Sci. Rep.* **2019**, *9* (1).

(46) Kolluru, C.; Gomaa, Y.; Prausnitz, M. R. Development of a Thermostable Microneedle Patch for Polio Vaccination. *Drug Deliv. Transl. Res.* **2019**, *9* (1), 192–203.

(47) Caffarel-Salvador, E.; Kim, S.; Soares, V.; Tian, R. Y.; Stern, S. R.; Minahan, D.; Yona, R.; Lu, X.; Zakaria, F. R.; Collins, J.; Wainer, J.; Wong, J.; McManus, R.; Tamang, S.; McDonnell, S.; Ishida, K.; Hayward, A.; Liu, X.; Hubálek, F.; Fels, J.; Vegge, A.; Frederiksen, M. R.; Rahbek, U.; Yoshitake, T.; Fujimoto, J.; Roxhed, N.; Langer, R.; Traverso, G. A Microneedle Platform for Buccal Macromolecule Delivery. *Sci. Adv.* **2021**, *7* (4).

(48) Ye, Y.; Wang, J.; Hu, Q.; Hochu, G. M.; Xin, H.; Wang, C.; Gu, Z. Synergistic Transcutaneous Immunotherapy Enhances Antitumor Immune Responses through Delivery of Checkpoint Inhibitors. ACS Nano 2016, 10 (9), 8956–8963.

(49) Fu, J.-J.; Li, C.-W.; Liu, Y.; Chen, M.-Y.; Zhang, Q.; Yu, X.-Y.; Wu, B.; Li, J.-X.; Du, L.-R.; Dang, Y.-Y.; Wu, D.; Wei, M.-Y.; Lin, Z.-Q.; Lei, X.-P. The Microneedles Carrying Cisplatin and IR820 to Perform Synergistic Chemo-Photodynamic Therapy against Breast Cancer. *J. Nanobiotechnology* **2020**, *18* (1).

(50) *P-type semiconductor*. Semicon-storage.com. https://toshiba.semicon-storage.com/ap-en/semiconductor/knowledge/e-learning/discrete/chap1/chap1-4.html (accessed 2024-04-30).

(51) *N-type semiconductor*. Semicon-storage.com. https://toshiba.semicon-storage.com/ap-en/semiconductor/knowledge/e-learning/discrete/chap1/chap1-3.html (accessed 2024-04-30).

(52) *Introduction to light emitting diodes.* Olympus-lifescience.com. https://www.olympus-lifescience.com/en/microscope-resource/primer/lightandcolor/ledsintro/ (accessed 2024-04-30).

(53) *History of LED lighting.* Shineretrofits.com. https://www.shineretrofits.com/lighting-center/lighting-resources/history-of-led-lighting/ (accessed 2024-04-30).

(54) Sparavigna, A. The Invention of Carborundum, the Synthetic Silicon Carbide. *Philica* **2018**.

(55) *Grainger Engineering Office of Marketing; Communications.* Nick Holonyak Jr., pioneer of LED lighting, dies. Illinois.edu. https://ece.illinois.edu/newsroom/51161 (accessed 2024-04-30).

(56) *What is LED - definition, working, properties, uses, advantages.* BYJUS. https://byjus.com/physics/light-emitting-diode/ (accessed 2024-04-30).

(57) *Types of LED: With classification, advantages, disadvantages.* Testbook. https://testbook.com/physics/types-of-led (accessed 2024-04-30).

(58) *Uses of LED: Learn practical applications of LED in real life.* Testbook. https://testbook.com/physics/uses-of-led (accessed 2024-04-30).

(59) Shi, X.; Zhang, H.; Jin, W.; Liu, W.; Yin, H.; Li, Y.; Dong, H. Metronomic Photodynamic Therapy with 5-Aminolevulinic Acid Induces Apoptosis and Autophagy in Human SW837 Colorectal Cancer Cells. *J. Photochem. Photobiol. B* **2019**, *198* (111586), 111586.

(60) Choi, J.; Lee, I. S.; Lee, J. S.; Jeon, S.; Yun, W. S.; Yang, S.; Moon, Y.; Kim, J.; Kim, J.; Choy, S.; Jeong, C.; Shim, M. K.; Kim, T.-I.; Kim, K. Implantable Micro-Scale LED Device Guided Photodynamic Therapy to Potentiate Antitumor Immunity with Mild Visible Light. *Biomater. Res.* **2022**, *26* (1).

(61) *MEETOPTICS.* Meetoptics.com. https://www.meetoptics.com/academy/light-emitting-diodes (accessed 2024-04-30).

CHAPTER 2

Fabrication of dissolvable microneedles patch

2.1 Introduction

Dissolvable microneedles (DMNs) operate using the simple "poke and release" principle[1], whereby the drug contained in the microneedle tips is released as soon as the microneedle penetrates the skin. There are many materials commonly used to create DMNs, such as gelatin[2,3], polyvinyl alcohol (PVA)[4], polyvinylpyrrolidone (PVP)[5], hyaluronic acid (HA)[6], and mono-disaccharide[7,8]. Each type of material has different physical characteristics and drug release rates, depending on the desired usage. DMNs that require rapid drug-release in the skin, mono-disaccharides are a common material option because of their hydrophilic characteristics, rapid solubility in water, and good mechanical strength. Mono-disaccharide-based DMNs will dissolve rapidly in the skin's interstitial fluids after application. Mono-disaccharides that have been reported to be used to fabricate DMNs such as sucrose[9], maltose[9-11], trehalose[9,12], and sorbitol[13,14].

Sorbitol is a sugar substitute obtained from the glucose-reducing process with the enzyme aldehyde/aldose reductase[15]. There have been reports of the formation of DMNs using sorbitol, for example the report from Kolluru et al.[13], they investigated the use of DMNs fabricated from a mixture of maltodextrin and D-sorbitol in histidine buffer for storage and delivery of polio vaccine (IPV) compared with conventional liquid IPV. The results demonstrated that commercial liquid IPV types 1 and 2 lost almost all activity in less than a month when stored at 40 °C, whereas IPV type 3 had less than 40% activity. In contrast, DMNs are more effective than traditional liquid IPV at preserving IPV activity. After two months and a year, all three IPV serotypes maintained >40% and >20% activity, respectively, at 40°C. Moreover, DMNs can rapidly deliver drugs to the skin. The needle dissolved within 15 minutes after inserting DMNs into a shaved porcine cadaver. Caffarel-Salvador et al.[14] investigated the use of polyvinylpyrrolidone-based MNs and sorbitol-based MNs to deliver human insulin (HI) through the palate and buccal mucosa of swine. The

results demonstrated that both kinds of DMN needles dissolved rapidly and delivered HI effectively. In the case of polyvinylpyrrolidone-based MNs, HI Cmax of 76 and 135 pM were observed after 40 to 50 min after application to the palate and buccal mucosa, respectively. Meanwhile, sorbitol-based MNs demonstrated higher variability when administered subcutaneously, with an HI concentration of up to 600 pM. HI Cmax of 111 and 130 pM were observed after 70 to 40 min after application to the palate and buccal mucosa, respectively. According to the research mentioned above, sorbitol has been demonstrated to be a desirable material for DMN creation due to its ability to maintain the active's quality while dissolving rapidly in the skin. Moreover, sorbitol is a sugar with a low glycemic index and has an antimicrobial effect. When sorbitol is fabricated as DMNs, it possesses not only the typical characteristics of DMNs made of mono-disaccharides but also the ability to have antibacterial properties and not raise users' blood sugar levels.[16,17]

There are now a number of techniques for creating DMNs, including droplet air blowing[18], drawing lithography[19], photopolymerization[19], and micromolding[19]. One of the most often used techniques for creating DMNs is micromolding, which is energy-efficient, portable, and capable of producing several workpieces at once.[20] The micromolding method involves placing the fluid material to be molded onto the microneedle mold. The material's fluid is then able to enter the microneedle mold once the air is removed by vacuuming the mold. The DMNs are subsequently peeled off the mold after drying.

In this study, the researcher therefore developed an interest in creating sorbitol-based DMNs using micromolding method with a 13 x 12 microneedle mold contained in a polydimethylsiloxane (PDMS) mold patch size of 12 × 11 mm. The drugs chlorin e6 (Ce6, photosensitizer), doxorubicin (DOX, chemotherapeutic drug), the combination of Ce6 and DOX, and methylene blue (MTB,

model drug) were loaded into sorbitol-based DMNs, and their various characteristics were then investigated.

2.2 Materials and methods

2.2.1 Preparation of silicone mold

The silicone rubber fluid (Rungart Resin Company, Thailand) was homogenously mixed with silicone crosslinker (1:1, 100 mL) before being poured into iron master molds (Mineed Technology, Thailand) and placed under vacuum for 5 min. The silicone-filled iron master molds were incubated at 100 ºC for 15 min. The crosslinked silicone molds were subsequently cooled to room temperature (25°C) before being peeled off the iron master molds.

2.2.2 Preparation of DMNs loading methylene blue (MTB-loaded DMNs)

The silicone molds were degased in DI water for 5 min before loading of MTB solution (10 mg mL^{-1} in distilled water, 22.3 µL) on silicone molds. The MTB-filled mold was placed in a light-proof box containing silica gel (AS ONE Corporation., Osaka, Japan) until it dried. The sorbitol solution (235% w/v in distilled water, 0.4 mL) was then dropped on the MTB-filled silicone and vacuumed for 2 min. The excess sorbitol solution on the silicone mold was cut off and placed in the light-proof and moisture-controlled chamber for 24 h. Then the bandage (1.2 x 1.2 cm) is placed on the mold and put them in the light-proof and moisture-controlled chamber for 48 h before peeling the DMNs from the silicone mold.

2.2.3 Preparation of DMNs loading chlorin e6, doxorubicin, or a combination of Ce6 and DOX (Ce6–, DOX–, or Ce6–DOX-loaded DMNs)

The silicone molds were degased in distilled water for 5 min before loading of Ce6 solution (2 mg mL^{-1} in ethanol, 90 µL) or/and DOX solution (1 mg mL^{-1} in distilled water, 43.2 µL). The drugs-

filled mold was placed in a light-proof box containing silica gel (AS ONE Corporation., Osaka, Japan) until dried. The sorbitol solution (235% w/v in DI water, 0.4 mL) was then dropped on the Ce6–, DOX–, or Ce6–DOX-filled silicone and vacuumed for 2 min. The excess sorbitol solution on the silicone mold was cut off and placed in the light-proof and moisture-controlled chamber for 24 h. Then the bandage (1.2 x 1.2 cm) is placed on the mold and put them in the light-proof and moisture-controlled chamber for 48 h before peeling the DMNs from the silicone mold.

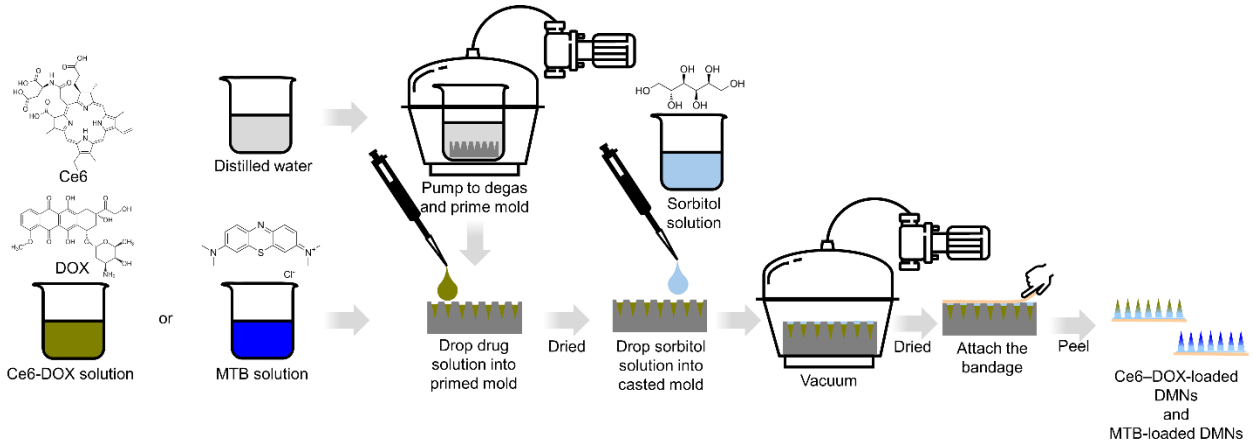

Figure 2.1 Schematic of DMN preparation using micromolding method.

2.2.4 Morphology of DMNs

The MTB-loaded DMNs and Ce6–DOX-loaded DMNs were kept in a light-proof box containing silica gel (AS ONE Corporation., Osaka, Japan) before being imaged by digital microscope (3R AnytyTM).

2.2.5 Drug loading efficiency

The total needles from Ce6-loaded DMNs and DOX-loaded DMNs were detached from the base and dissolved in ethanol and DI water, respectively. The needle solutions were evaluated using a fluorescence spectrometer to determine the concentration of Ce6 or DOX, comparing the standard solution curves. The drug loading amount was calculated according to the following equation:

$$\text{Loading efficiency} = \frac{\text{Amount of loaded drug in the needles (μg)}}{\text{Amount of drug used to load (μg)}} \times 100$$

2.2.6 Mechanical properties

Ce6–DOX-loaded DMNs were carried out using the universal testing machine (UTM, Shimadzu EZ-S, Shimadzu Corporation, Tokyo, Japan). These DMNs were analyzed using a compressor with a diameter of 1.5 cm at the constant crosshead speed of 1.0 mm min^{-1}. The displaced distance was recorded along with the compressive force with the maximum compressive force set at 400 N. The measurement was stopped when the compressor reached the maximum force. The mechanical results are divided by the total number of needles to examine the force per needle.

2.2.7 *In vitro* efficacy of drug delivery

Franz diffusion cell was used to carry out the released MTB from MTB-loaded DMNs. Briefly, phosphate buffer saline (pH 7.4, 10 mL) was used as the receptor medium, which was controlled at 37°C and continuously stirred by a magnetic stirrer. MTB-loaded DMNs were pressed and mounted on the porcine skin. At different time points (3 h, 6 h, 12 h, and 24 h), incubated solution (1 mL) was taken out and replaced with an equal volume of phosphate buffer saline (pH 7.4). The taken-out solutions were evaluated using UV-visible spectrometer to determine the released MTB comparing standard solution curve (Figure 2.4). To evaluate released MTB from MTB solution alone or MTB solution with Tween 80 (5% v/v) solution, the solutions were applied on porcine skin and performed the same experiment as the MTB-loaded DMNs's experiment. All experiments were performed in triplicate. The delivery efficiency was calculated according to the following equation:

$$\text{Delivery efficiency} = \frac{\text{Amount of released MTB (μg)}}{\text{Amount of MTB in the patch/gel (μg)}} \times 100$$

2.2.8 *Ex vivo* efficacy of drug delivery

To evaluate the diffusion of MTB-loaded DMNs in porcine skin, fresh porcine skin was placed on the phosphate buffer saline (pH 7.4) at controlled temperature (37 °C) for 15 min. Then, MTB-loaded DMNs were pressed for 10 s and mounted with plastic tape. The DMNs-pressed skin was placed on phosphate buffer saline (pH 7.4) at 37 °C. At different time points (0, 5, 10, 20, 30, 60, 90, 120, 150, and 180 min), the DMNs-pressed skin was surgically sectioned, and the tissue section was examined under digital microscope (3R AnytyTM). To evaluate the diffusion of MTB solution alone or MTB with Tween 80 (5% v/v) solution in porcine skin, fresh porcine skin was placed on the phosphate buffer saline (pH 7.4) at controlled temperature (37 °C) for 15 min. Then, skin was gently treated with MTB solution alone or MTB with Tween 80 (5% v/v) solution and performed the same experiment as the MTB-loaded DMNs's experiment.

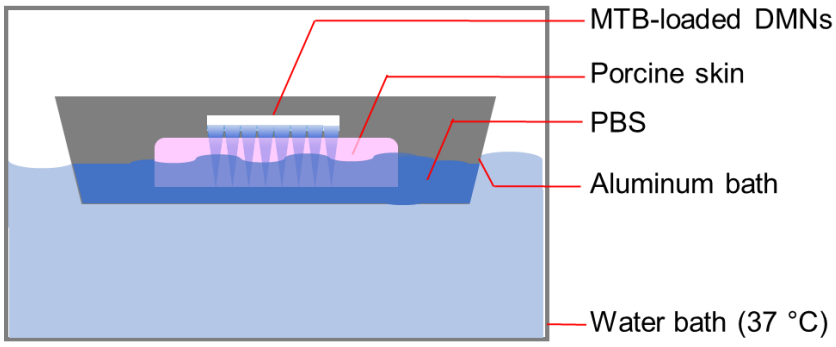

Figure 2.2 *Ex vivo* investigation of drug distribution in porcine skin.

2.2.9 Statistic analysis

Every experiment was carried out in triplicate and repeated three or more times. Quantitative values are demonstrated as the mean ± standard deviation (SD) of at least three independent experiments. Statistical differences were performed by the one-way analysis of variance

(ANOVA). P-values <0.05 were considered significant, and P-values <0.01 were considered highly significant.

2.3 Results and discussion

2.3.1 Fabrication and characterization of Ce6–DOX-loaded DMNs and MTB-loaded DMNs

DMNs loading chlorin e6 and doxorubicin (Ce6–DOX-loaded DMNs) and DMNs loading methylene blue (MTB-loaded DMNs) have been successfully fabricated via micromolding process (Figure 2.3). Both Ce6–DOX-loaded DMNs and MTB-loaded DMNs have dimensions of 12 x 11 mm containing an array of 13×12 needles. The needles are rectangular prism with a pyramid on top. The average height of the needle is 1000 µm, with the height of pyramid part and prism part of 600 µm and 400 µm, respectively. The size of the needle-base is 300x300 µm which located on half circle with a diameter of 300 µm. The tip-to-tip distance of 1000 µm. The majority of drugs are loaded at the tip of needles. This assists in delivering the drug to the skin's deeper layers when implanted into the skin.

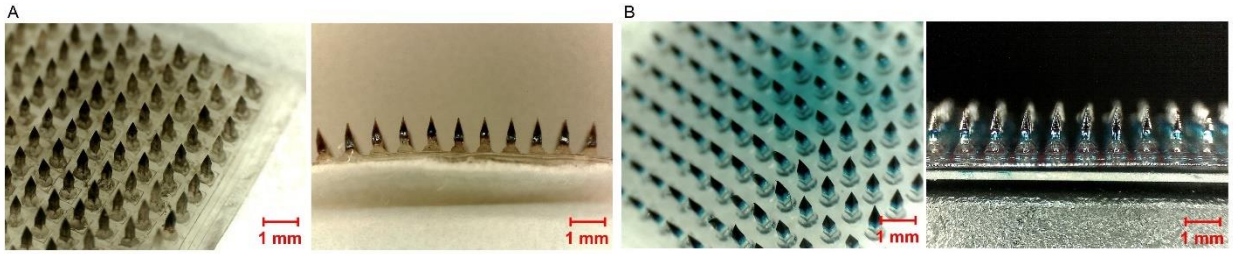

Figure 2.3 Morphology of A) Ce6–DOX-loaded DMNs and B) MTB-loaded DMNs.

2.3.2 Drug loading efficiency

Ce6-loaded DMNs and DOX-loaded DMNs were scraped off only the needle part. The Ce6 needles and DOX needles were then dissolved in ethanol and distilled water, respectively. The emission of the Ce6 needle solution and the DOX needle solution was measured comparing

standard solutions using a fluorescence spectrometer at 667 nm and 593 nm as shown in Figure 2.4, respectively. The results demonstrate that the micromolding method for creating DMNs yields the encapsulation efficiency of Ce6 and DOX at 91.12% and 86.37%, respectively.

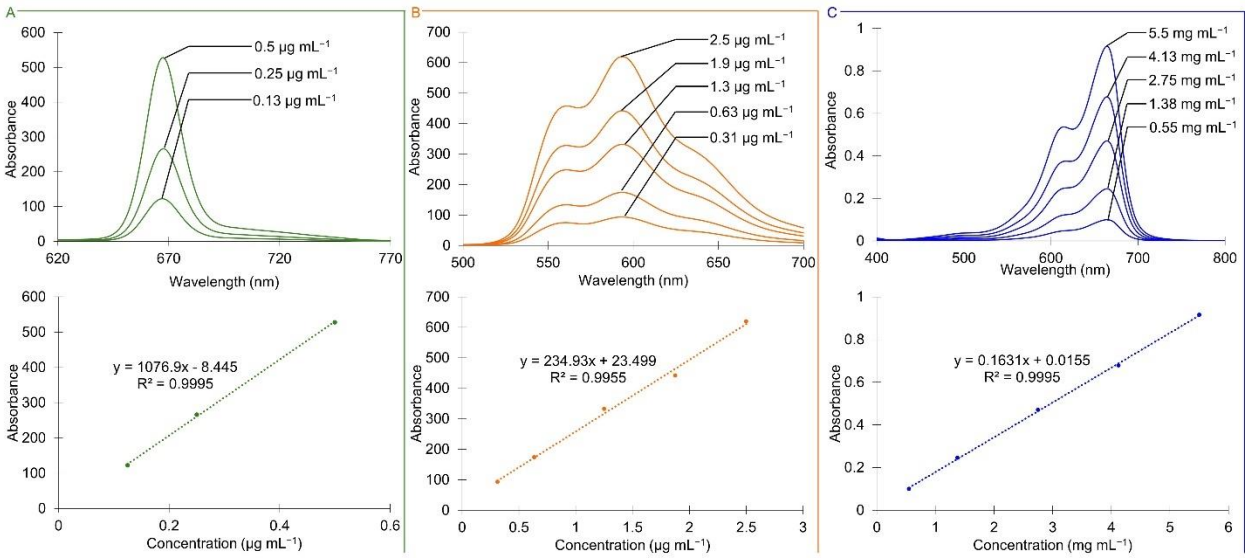

Figure 2.4 Relationship between concentration and absorbance, and calibration curve of A) Ce6, B) DOX, and C) MTB standard solutions.

2.3.3 Mechanical properties

The mechanical properties of three Ce6–DOX-loaded DMNs were measured using the universal testing machine. The results demonstrate that Ce6–DOX-loaded DMNs have a force tolerance of 1.34 N/needle (Figure 2.5), which is greater than the minimal force tolerance of 0.345 N/needle required for MN implantation into the mammalian skin.

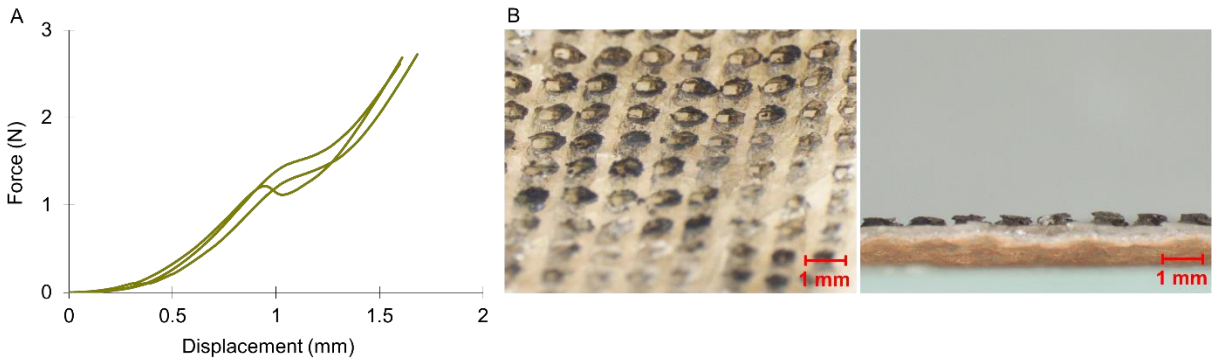

Figure 2.5 Mechanical measurement of Ce6–DOX-loaded DMNs. A) Graphs of displaced distances and applied forces of Ce6–DOX-loaded DMNs and B) photos of Ce6–DOX-loaded DMNs after mechanical compression.

2.3.4 *In vitro* efficacy of drug delivery

MTB was used as a model drug to study drug release profiles using the Franz cell technique. The study examined three different types of drug delivery through the skin: applying MTB solution alone, applying MTB solution mixed with Tween 80 (5% v/v), and implanting MTB-loaded DMNs on porcine skin. The results are demonstrated in Figure 2.6. After 3 h of application, the drug solution or the drug mixing the penetration enhancer (Tween 80) had drug delivery efficiencies of 3.21% and 4.93%, respectively. Even after 24 h, only 14.17% and 17.77% of the drug could be delivered into the medium, respectively. Meanwhile, using MBT-loaded DMNs, even after only 3 h, the drug can be delivered up to 11.92%, which improves the efficiency of drug delivery into the skin more than two times compared to topical application. After the 24-h period has passed, the drug can be delivered up to 32.56%. Thus, it may be concluded that the use of DMNs results in a better efficiency of drug delivery into the skin than drug delivery in the form of topical application.

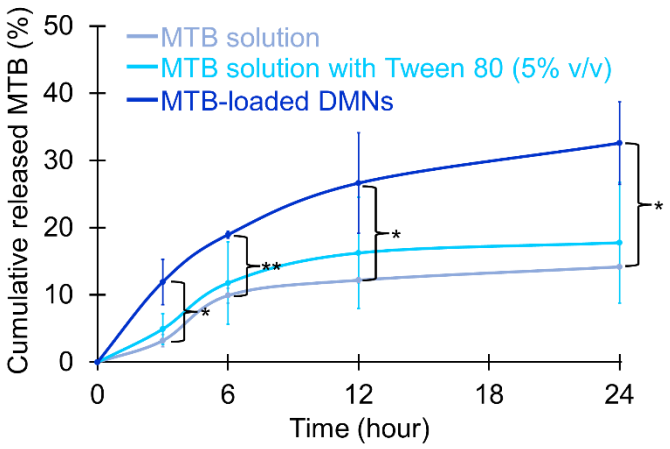

Figure 2.6 *In vitro* cumulative released MTB using Franz cell technique. Data are expressed as means ± standard error of the mean (SEM) (n=3). Significance was assessed using one-way analysis of variance (ANOVA); **$p < 0.01$ and *$p < 0.05$.

2.3.5 *Ex vivo* efficacy of drug delivery

The MTB distribution in the skin of the three different types of samples was examined by cross-section using a digital microscope at various times. As demonstrated in Figure 2.7, applying the MTB either as a MTB solution alone or as a MTB mixed with Tween 80 reveals minimal absorption and distribution of MBT in the skin. The majority of the MBT remained on the skin. In the meantime, MBT can be delivered intradermally into deeper layers using MTB-loaded DMNs. The MTB distribution was evidently widespread and deep in the porcine skin over the same period of time. As a result, it may be argued that using DMNs to deliver drugs into the skin results in a more effective drug distribution and delivery than applying drugs topically.

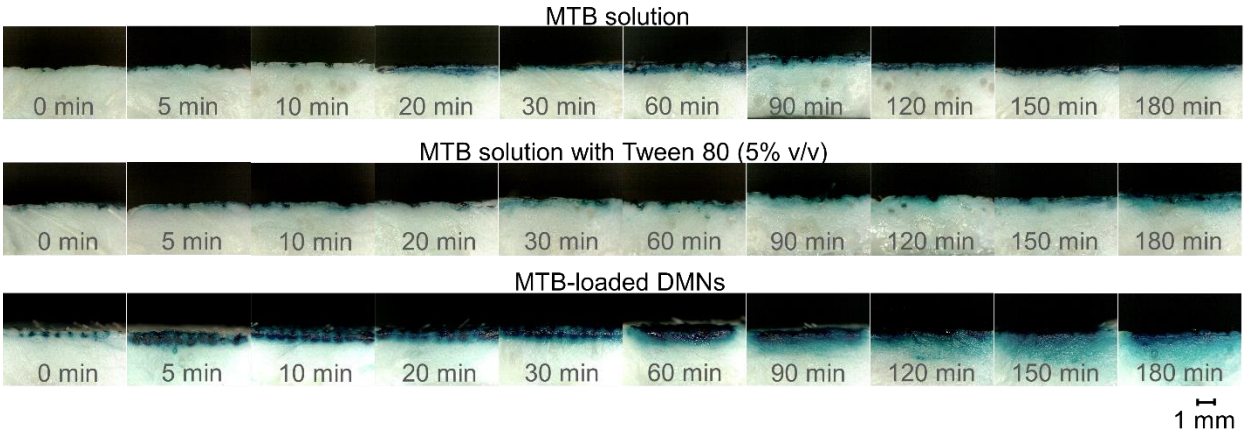

Figure 2.7 *Ex vivo* MTB distribution in porcine skin.

2.4 Conclusion

A simple micromolding method was used to successfully fabricate Ce6-, DOX-, Ce6–DOX-, and MTB-loaded DMNs. The majority of the drugs were located at the needle's tip, with the encapsulation of Ce6 and DOX of 91.12% and 86.37%, respectively. The 12 x 11 mm moldable DMN containing 13 x 12 micron needles, each with a height of 1000 μm. The Ce6–DOX-loaded DMNs can withstand a pressure of up to 1.34 N/needle, which is strong enough to penetrate mammalian skin. By implanting DMNs into porcine skin to investigate drug release and drug distribution using MTB as a model drug, DMNs were found to significantly increase drug delivery and distribution in the skin when compared to applying MTB solution alone or MTB solution with Tween 80 (5% v/v). In a 24-hour period, DMNs were able to improve drugs penetration into the skin by 32.56%, whereas using MTB solution alone or in combination with Tween 80 had penetration percentages of only 14.17% and 17.77%, respectively.

2.5 References

(1) Ita, K. Dissolving Microneedles for Transdermal Drug Delivery: Advances and Challenges. *Biomed.Pharmacother.* **2017**, *93*,1116–1127.

(2) Ryota, N.; Hirofumi, M.; Shigeki, T. A Novel Microneedle Device Having Flexible Substrate and Strong Needles Using PVA and Gelatin. In *2017 International Symposium on Micro-NanoMechatronics and Human Science (MHS)*; IEEE, **2017**.

(3) Chiu, T.-M.; Hsu, P.-C.; Khan, M. Y.; Lin, C.-A. J.; Lee, C.-H.; Hsu, T.-C.; Chen, M.-H.; Hanagata, N. A Perspective on Imiquimod Microneedles for Treating Warts. *Pharmaceutics* **2021**, *13* (5), 607.

(4) Terashima, S.; Tatsukawa, C.; Suzuki, M.; Takahashi, T.; Aoyagi, S. Twice Stretched Fabrication of Polylactic Acid Microneedle Arrays Using Drawing Lithography. *Int. J. Precis. Eng. Manuf.* **2020**, *21* (10), 1933–1942.

(5) Lee, C.; Kim, J.; Um, D. J.; Kim, Y.; Min, H. S.; Shin, J.; Nam, J. H.; Kang, G.; Jang, M.; Yang, H.; Jung, H. Optimization of Layered Dissolving Microneedle for Sustained Drug Delivery Using Heat-Melted Poly(Lactic-Co-Glycolic Acid). *Pharmaceutics* **2021**, *13* (7), 1058.

(6) Fakhraei Lahiji, S.; Kim, Y.; Kang, G.; Kim, S.; Lee, S.; Jung, H. Tissue Interlocking Dissolving Microneedles for Accurate and Efficient Transdermal Delivery of Biomolecules. *Sci. Rep.* **2019**, *9* (1).

(7) Kolluru, C.; Gomaa, Y.; Prausnitz, M. R. Development of a Thermostable Microneedle Patch for Polio Vaccination. *Drug Deliv. Transl. Res.* **2019**, *9* (1), 192–203.

(8) Caffarel-Salvador, E.; Kim, S.; Soares, V.; Tian, R. Y.; Stern, S. R.; Minahan, D.; Yona, R.; Lu, X.; Zakaria, F. R.; Collins, J.; Wainer, J.; Wong, J.; McManus, R.; Tamang, S.; McDonnell, S.; Ishida, K.; Hayward, A.; Liu, X.; Hubálek, F.; Fels, J.; Vegge, A.; Frederiksen, M. R.; Rahbek, U.; Yoshitake, T.; Fujimoto, J.; Roxhed, N.; Langer, R.; Traverso, G. A Microneedle Platform for Buccal Macromolecule Delivery. *Sci. Adv.* **2021**, *7* (4).

(9) Loizidou, E. Z.; Williams, N. A.; Barrow, D. A.; Eaton, M. J.; McCrory, J.; Evans, S. L.; Allender, C. J. Structural Characterisation and Transdermal Delivery Studies on Sugar Microneedles: Experimental and Finite Element Modelling Analyses. *Eur. J. Pharm. Biopharm.* **2015**, *89*, 224–231.

(10) Toprangkobsin, P.; Banlunara, W.; Limcharoen, B.; Leelahavanichkul, A.; Asawanonda, P.; Kumtornrut, C.; Sansureerungsikul, T.; Rutwaree, T.; Wanichwecharungruang, S. Delivery and Diffusion of Retinal in Dermis and Epidermis through the Combination of Prodrug Nanoparticles and Detachable Dissolvable Microneedles. *Research Square*, **2021**.

(11) Toprangkobsin, P.; Banlunara, W.; Limcharoen, B.; Leelahavanichkul, A.; Asawanonda, P.; Kumtornrut, C.; Sansureerungsikul, T.; Rutwaree, T.; Wanichwecharungruang, S. Delivery and Diffusion of Retinal in Dermis and Epidermis through the Combination of Prodrug Nanoparticles and Detachable Dissolvable Microneedles. *Drug Deliv. Transl. Res*. **2022**, *12* (11), 2751–2761.

(12) Kim, H. K.; Lee, S. H.; Lee, B. Y.; Kim, S. J.; Sung, C. Y.; Jang, N. K.; Kim, J. D.; Jeong, D. H.; Ryu, H. Y.; Lee, S. A Comparative Study of Dissolving Hyaluronic Acid Microneedles with Trehalose and Poly(Vinyl Pyrrolidone) for Efficient Peptide Drug Delivery. *Biomater. Sci.* **2018**, *6* (10), 2566–2570.

(13) Kolluru, C.; Gomaa, Y.; Prausnitz, M. R. Development of a Thermostable Microneedle Patch for Polio Vaccination. *Drug Deliv. Transl. Res.* **2019**, *9* (1), 192–203.

(14) Caffarel-Salvador, E.; Kim, S.; Soares, V.; Tian, R. Y.; Stern, S. R.; Minahan, D.; Yona, R.; Lu, X.; Zakaria, F. R.; Collins, J.; Wainer, J.; Wong, J.; McManus, R.; Tamang, S.; McDonnell, S.; Ishida, K.; Hayward, A.; Liu, X.; Hubálek, F.; Fels, J.; Vegge, A.; Frederiksen, M. R.; Rahbek, U.; Yoshitake, T.; Fujimoto, J.; Roxhed, N.; Langer, R.; Traverso, G. A Microneedle Platform for Buccal Macromolecule Delivery. *Sci. Adv.* **2021**, *7* (4).

(15) Ramana, K. V.; Srivastava, S. K. Aldose Reductase: A Novel Therapeutic Target for Inflammatory Pathologies. *Int. J. Biochem. Cell Biol.* **2010**, *42* (1), 17–20.

(16) Tiefenbacher, K. F. Technology of Main Ingredients—Sweeteners and Lipids. In *Wafer and Waffle*; Elsevier, **2017**; pp 123–225.

(17) Chan, A.; Ellepola, K.; Truong, T.; Balan, P.; Koo, H.; Seneviratne, C. J. Inhibitory Effects of Xylitol and Sorbitol on Streptococcus Mutans and Candida Albicans Biofilms Are Repressed by the Presence of Sucrose. *Arch. Oral Biol.* **2020**, *119* (104886), 104886.

(18) Kim, J. D.; Kim, M.; Yang, H.; Lee, K.; Jung, H. Droplet-Born Air Blowing: Novel Dissolving Microneedle Fabrication. *J. Control. Release* **2013**, *170* (3), 430–436.

(19) Hao, Y.; Li, W.; Zhou, X.; Yang, F.; Qian, Z. Microneedles-Based Transdermal Drug Delivery Systems: A Review. *J. Biomed. Nanotechnol.* **2017**, *13* (12), 1581–1597.

(20) Scott, S.; Ali, Z. Fabrication Methods for Microfluidic Devices: An Overview. *Micromachines (Basel)* **2021**, *12* (3), 319.

CHAPTER 3

Cell viability assay

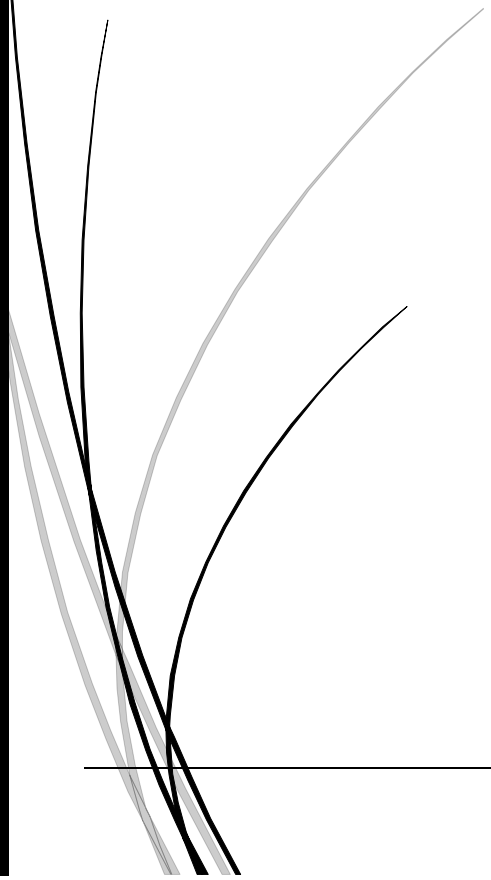

3.1 Introduction

Colon-26 is a mouse colon cancer cell line produced from the tumor tissue of Balb/c mice bearing Colon-26 carcinoma, generated by a single rectal administration of N-nitroso-N-methyl-urethan (NMU).[1,2] Colon-26 is typically cultured in RPMI 1640 supplemented with 10% FBS and rises in 15 to 20 hours. The Colon-26 cells were used to produce the cachectic mouse model for the purpose of studying cancer cachexia, a syndrome characterized by a gradual loss of skeletal muscle mass and adipose tissue that results in weight loss and weakness.[1] Following Colon-26 cell inoculation, the transplanted mice developed the following syndromes: hypoglycemia, hypercorticism, prolonged and significant weight loss as tumor progression, and abnormalities of hepatic functioning. As the Colon-26 tumor grew, muscular cross-sectional area and muscular strength decreased, and skeletal muscle and adipose tissues were gradually eliminated. The loss of muscle tissue caused by the Colon-26 tumor might be related to the activation of proteolytic mechanisms in skeletal muscle.[1-3] To eliminate Colon-26 or other cancer cell lines in cachectic mice models, many anticancers have been used in several studies. The drugs were investigated, including photosensitizers and chemotherapy drugs.[4-7]

B16F10 melanoma is a murine (mouse) cell line extensively used in cancer research, particularly in studies related to melanoma, a severe form of skin cancer.[8] The B16F10 cells came from a spontaneous melanoma in C57BL/6 mice. They are known to be aggressive and have a high ability to metastasize, which makes them a useful tool for studying cancer biology and possible treatments.[9] B16F10 melanoma cells exhibit rapid growth and the ability to metastasize to various organs, including the lungs, liver, and spleen, mimicking the behavior of human melanoma.[10] This property allows researchers to study not only primary tumor development but also the mechanisms underlying metastasis, which is a critical aspect of cancer progression and patient prognosis.

Photosensitization is the fundamental principle of photon absorption and subsequent energy transfer. Photosensitizers are molecules capable of absorbing photons of specific wavelengths, typically within the ultraviolet or visible spectrum. Upon absorption, these molecules undergo a transition to an excited state, characterized by increased energy levels. This energy can then be transferred to adjacent molecules, initiating diverse photochemical processes.[11,12] There are various mechanisms of photosensitizer, depending on their specific properties and the target application.[13,14] In photodynamic therapy (PDT) to eliminate cancer tumors, photosensitizers are administered to selectively target cancer tumors. Upon exposure to light of an appropriate wavelength, these sensitizers generate reactive oxygen species (ROS) through a series of photochemical reactions. ROS, such as superoxide (O_2^-), hydroxyl radical ($OH^\bullet$), singlet oxygen, and hydrogen peroxide (H_2O_2), inflict oxidative damage to cellular components, ultimately leading to cell death or apoptosis.[15,16] This precise localization of phototoxicity enables PDT to selectively eradicate cancerous cells while minimizing damage to healthy tissue. There are many photosensitizers that are certified by the Food and Drug Administration (FDA) for cancer treatment, such as porfimer sodium, temoporfin, motexafin lutetium, and chlorin e6.[17]

Chlorin e6 (Ce6) is a naturally occurring porphyrin derivative belonging to the family of chlorophyll-related compounds. Its molecular structure comprises four pyrrole rings interconnected by methine bridges, forming a tetrapyrrole macrocycle.[18] This structure confers chlorin e6 with unique optical and chemical properties, making it an ideal candidate for photodynamic therapy and other photomedicine applications. One of the notable features of chlorin e6 is its absorption spectrum, which extends into the red region of the electromagnetic spectrum.[19] This characteristic allows chlorin e6 to effectively absorb light with longer wavelengths, enabling deeper tissue penetration compared to photosensitizers with absorption predominantly in the blue

or green regions. Moreover, chlorin e6 exhibits strong fluorescence properties, emitting light upon excitation by an external light source. This fluorescence phenomenon serves not only as a diagnostic tool for detecting the presence of chlorin e6 in tissues but also contributes to its therapeutic efficacy by enhancing the generation of reactive oxygen species (ROS) during photodynamic therapy. Applications of chlorin e6 include cancer therapy, antimicrobial treatment, and diagnostic imaging.[20,21]

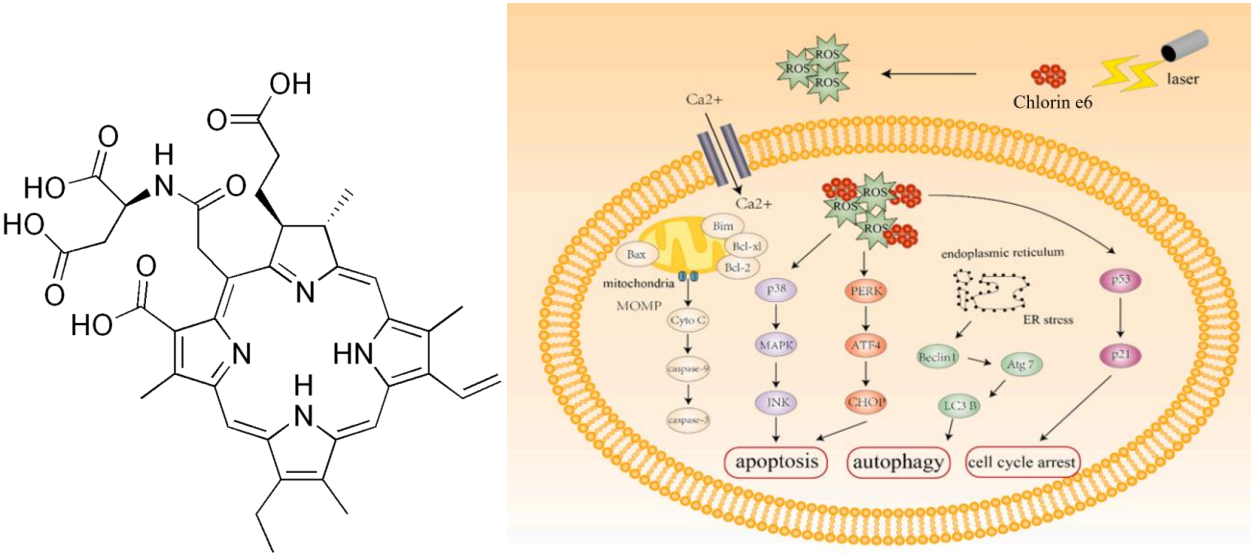

Figure 3.1 Structural formula of chlorin e6 and its anticancer mechanism through various pathways.[22]

Chemotherapeutic drugs employ a diverse array to combat malignant cells and inhibit tumor growth.[23] These drugs exert their effects through various mechanisms, which can be broadly categorized as including interference with DNA synthesis, induction of apoptosis, inhibition of cell signaling pathways, and disruption of the tumor microenvironment.[24] Chemotherapeutic drugs encompass a broad spectrum of agents with diverse chemical structures, mechanisms of action, and therapeutic indications. Some of the major classes of chemotherapeutic drugs include interference of DNA replication and transcription (cyclophosphamide, cisplatin, and

temozolomide), interference of nucleic acid synthesis (methotrexate, 5-fluorouracil (5-FU), and gemcitabine), disruption of microtubule assembly (paclitaxel, vincristine, and docetaxel), specific inhibition of molecular mechanisms involved in cancer growth and progression; tyrosine kinase inhibitors (imatinib and erlotinib); monoclonal antibodies (trastuzumab and rituximab); proteasome inhibitors (bortezomib), topoisomerase inhibitors (etoposide, irinotecan, and doxorubicin).[25,26]

From the chemotherapy drugs already described, doxorubicin (DOX), is one of the chemotherapeutic drugs commonly used in cancer treatment because it exhibits broad-spectrum activity against various types of cancer and long-term survival benefits, including reduced risk of disease recurrence and prolonged progression-free survival.[27,28] Doxorubicin, a member of the anthracycline class of chemotherapeutic agents, stands as a cornerstone in the treatment of various cancers. Doxorubicin exerts its anticancer effects through multiple mechanisms, targeting critical pathways involved in cell proliferation, DNA synthesis, and cellular metabolism.[29]

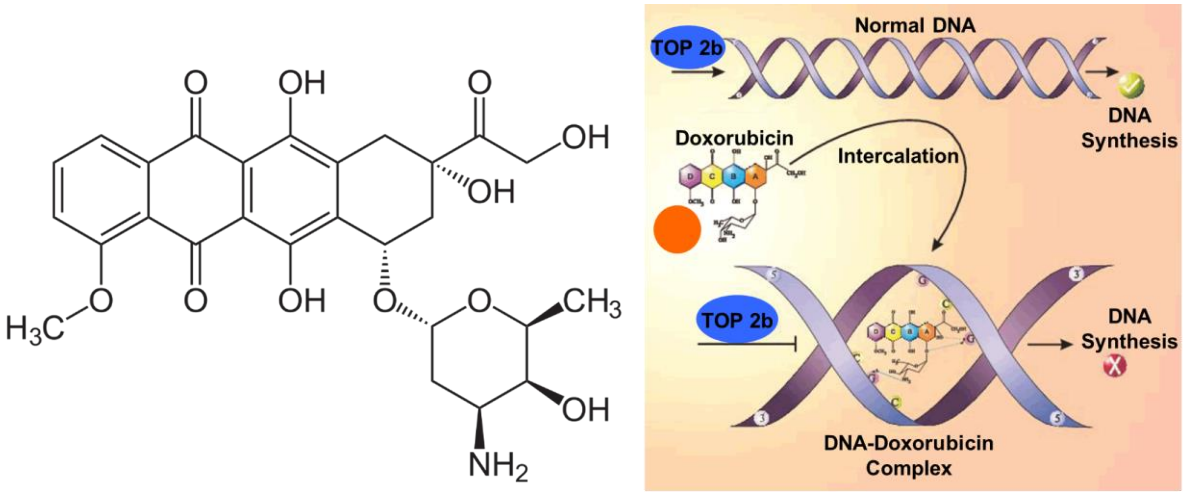

Figure 3.2 The structural formula of doxorubicin and its anticancer mechanism through DNA synthesis.[29]

For these reasons, the researcher in this study investigated the removal of Colon-26 cells and B16F10 melanoma cells using Ce6, DOX, and a combination of Ce6 and DOX. The effectiveness of each drug type in eradicating Colon-26 cells and B16F10 melanoma cells was investigated under both light and dark conditions.

3.2 Cell culture and cell viability assays

The Colon-26 cells or B16F10 melanoma cells were cultivated in Roswell Park Memorial Institute 1640 Medium (Gibco, Grand Island, NY) containing 10% fetal bovine serum, L-glutamine (2mM), sodium pyruvate (1mM), gentamycin, and penicillin-streptomycin (100 IU mL^{-1}), following the manufacturer's suggested methodology. Cells were seeded at 7000 cells per well in 96-well tissue culture plates at 37 °C in a humidified incubator containing 5% CO_2 and left to adhere throughout the entire night. The cells were then incubated for 48 h with various concentrations of drugs under the same conditions. The cells were then washed with phosphate buffer saline (pH 7.4) and incubated for 3 h at 37 °C with the Cell Counting Kit-8 solution (CCK-8; Dojindo Laboratories, Kumamoto, Japan). The orange formazan products were measured at the absorbance of 450/690 nm was determined to analyze the living-cell using a microplate reader (Infinite M200 PRO; Tecan, Männedorf, Switzerland).

3.3 Cellular experiment conditions

3.3.1 The Ce6 and DOX concentration on cell viability under dark, red LED shining, and white LED shining

Following well growth and adhesion of Colon-26 cells or B16F10 melanoma cells in the 96-well cell culture plates, both cells were rinsed with PBS and incubated for 48 hours at different concentrations of either DOX (100, 50, 25, 12.5, 6.3, 3.1, 1.6, 0.8, 0.4, 0.2, 0.1, 0.05, and 0.02 µg

mL^{-1}) or Ce6 (100, 50, 25, 12.5, 6.3, 3.1, 1.6, 0.8, 0.4, 0.2, 0.1, 0.05, and 0.02 µg mL^{-1}). Before cell incubation accomplished 48-hour maturity, red or white LEDs were placed on 96-well cell culture plates and left exposed for 15 minutes (Figure 3.3). Then, the cells were washed with phosphate buffer saline (pH 7.4) and incubated with the Cell Counting Kit-8 solution (CCK-8; Dojindo Laboratories, Kumamoto, Japan) for 3 h at 37 °C under humidified chamber containing 5% CO_2. The orange formazan products were measured at the absorbance of 450/690 nm was determined to analyze the living-cell using a microplate reader (Infinite M200 PRO; Tecan, Männedorf, Switzerland).

3.3.2 The combination of Ce6 and DOX on cell viability

Following well growth and adhesion of Colon-26 cells or B16F10 melanoma cells in the 96-well cell culture plates, both Colon-26 cells or B16F10 melanoma cells were rinsed with PBS and incubated for 48 hours under various combinations of Ce6 and DOX at different concentration ratios [Ce6 (µg mL^{-1}) : DOX (µg mL^{-1}) = 1.6 : 1.6, 1.6 : 0.8, 1.6 : 0.4, 1.6 : 0.2, 0.8 : 1.6, 0.8 : 0.8, 0.8 : 0.4, 0.8 : 0.2, 0.4 : 1.6, 0.4 : 0.8, 0.4 : 0.4, 0.4 : 0.2, 0.2 : 1.6, 0.2 : 0.8, 0.2 : 0.4, and 0.2 : 0.2]. Before cell incubation accomplished 48-hour maturity, white LEDs were placed on 96-well cell culture plates and left exposed for 15 minutes. Then, the cells were washed with phosphate buffer saline (pH 7.4) and incubated with the Cell Counting Kit-8 solution (CCK-8; Dojindo Laboratories, Kumamoto, Japan) for 3 h at 37 °C under humidified chamber containing 5% CO_2. The orange formazan products were measured at the absorbance of 450/690 nm was determined to analyze the living-cell using a microplate reader (Infinite M200 PRO; Tecan, Männedorf, Switzerland).

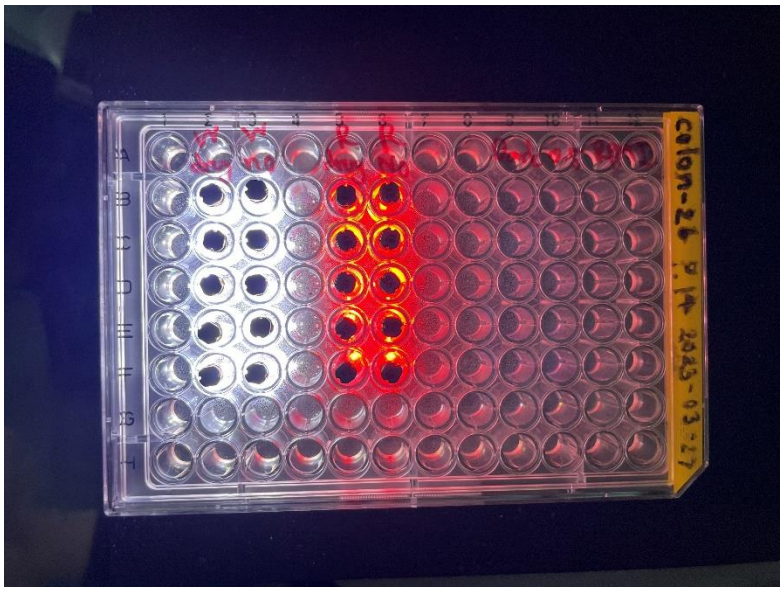

Figure 3.3 Cellular experiment with wireless LED system.

3.4 Statistic analysis

Every experiment was carried out five times. Quantitative values are demonstrated as the mean ± standard deviation (SD) (n = 5) of at least five independent experiments. Statistical differences were performed by the one-way analysis of variance (ANOVA). P-values <0.05 were considered significant.

3.5 Results and discussions

3.5.1 The Ce6 and DOX concentration on Colon-26 viability under dark, red LED shining, and white LED shining

Ce6 and DOX concentrations affect Colon-26 cell viability under dark, red, and white light conditions, as determined by the MTS assay 48 hours after various drug concentrations were introduced. Ce6 concentration's influence on Colon-26 cell viability (Figure 3.4A) demonstrated that under dark, white LED, and red LED lighting, cell viability tended to decrease as Ce6 concentrations increased. In addition, the results demonstrated that the combination of red and

white LED shining was more effective at eradicating Colon-26 cells compared to when there was no light. However, when red LED and white LED were compared, the results demonstrated that at lower Ce6 concentrations, white LED was shown to be substantially more effective than red LED in stimulating Ce6 to generate ROS, which in turn eradicated Colon-26 cells. Resulting in lower Colon-26 cell viability.

The effect of DOX concentration on Colon-26 cell viability was examined (Figure 3.4B), and it was discovered that a higher DOX concentration was associated with a reduction in Colon-26 cell viability. Red and white LED irradiation were found to have no effect on the effectiveness of DOX in eradicating Colon-26 cells when compared to no irradiation at all concentrations. This result may be due to the fact that DOX is a chemotherapeutic drug and does not require light to activate like a photosensitizer. Consequently, DOX's ability to eradicate Colon-26 at all concentrations was unaffected by either red LED or white LED irradiation.

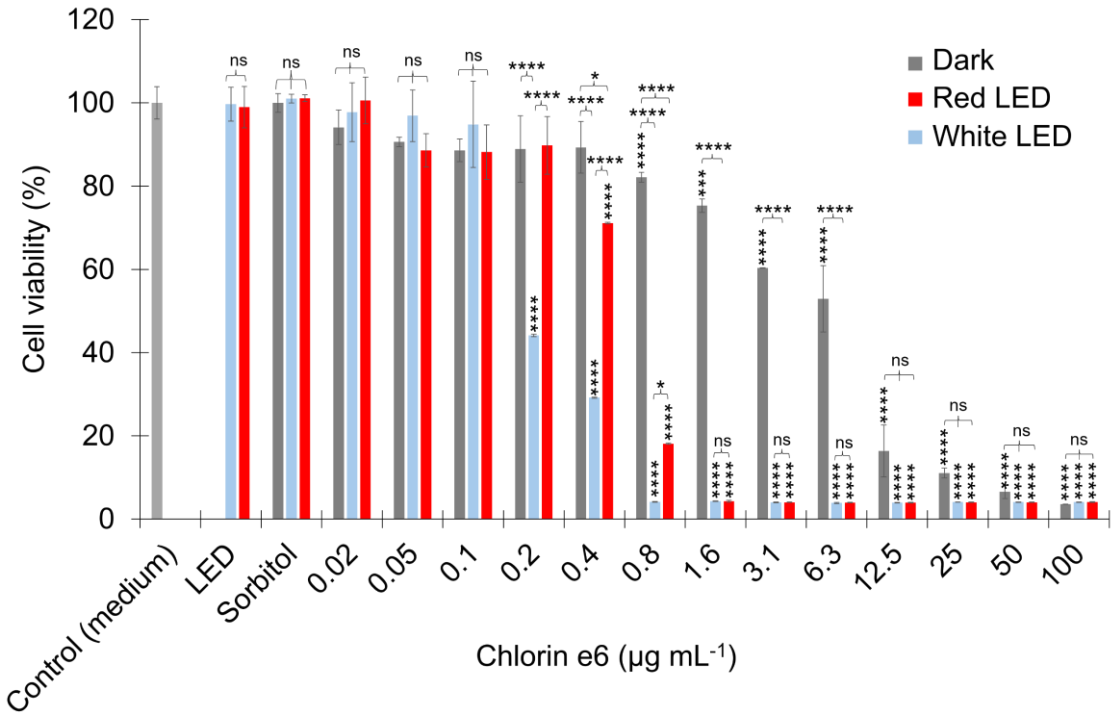

(A)

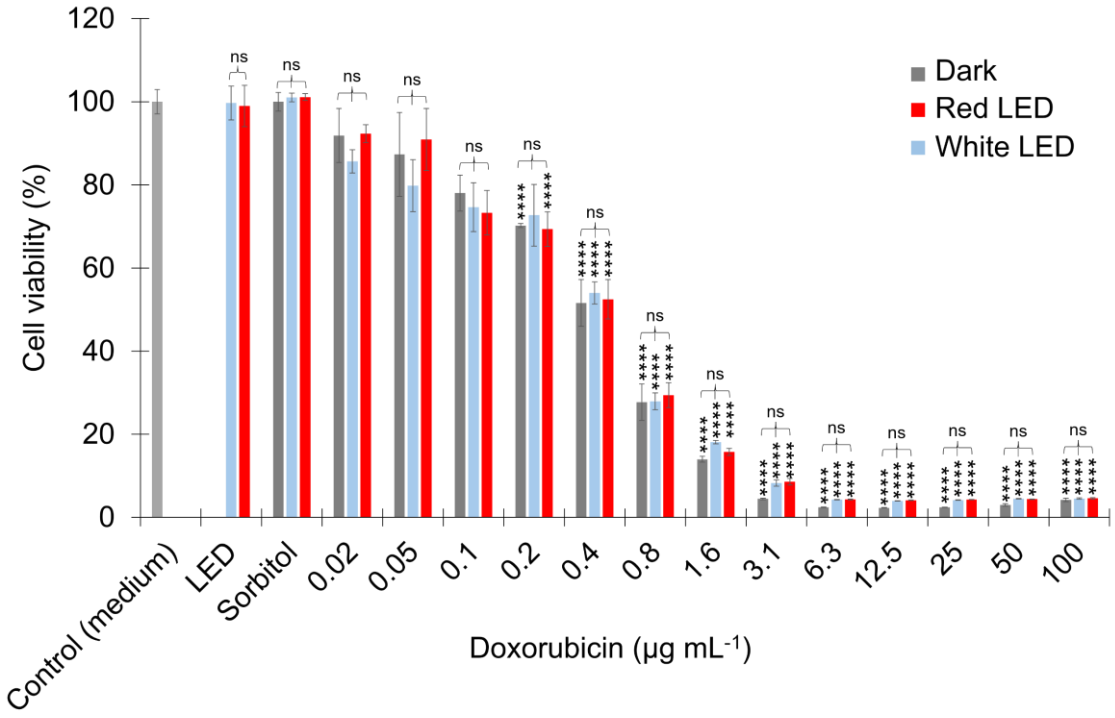

(B)

Figure 3.4 *In vitro* viability of Colon-26 cells treated with A) Ce6 and B) DOX (under dark, red LED shining, and white LED shining) including red LED, white LED, and sorbitol (5 mg mL^{-1}). Data are expressed as means ± standard error of the mean (SEM) (n = 5). Statistical analysis was assessed using one-way ANOVA followed by Tukey's test; ****, $p < 0.0001$; ***, $p < 0.001$; **, $p < 0.01$; *, $p < 0.05$.

3.5.2 The Ce6 and DOX concentration on B16F10 melanoma cell viability under dark, red LED shining, and white LED shining

Ce6 and DOX concentrations on B16F10 melanoma cell viability under dark, red, and white light conditions, as determined by the MTS assay 48 hours after various drug concentrations were introduced. The effect of Ce6 concentration on B16F10 melanoma cell viability (Figure 3.5A) revealed that cell viability tended to decrease as Ce6 concentrations increased under dark, white

LED, and red LED lighting. In addition, the results demonstrated that the combination of red and white LED shining was more effective at eradicating B16F10 melanoma cells compared to when there was no light. However, when red LED and white LED were compared, the results demonstrated that at lower Ce6 concentrations, white LED was shown to be substantially more effective than red LED in stimulating Ce6 to generate ROS, which in turn eradicated B16F10 melanoma cells. Resulting in lower cell viability.

The white LED was more effective than the red LED in activating Ce6 and eradicating both Colon-26 cells and B16F10 melanoma cells, which could be attributed because Ce6 can absorb light in the 320–420 and 650–690 nm ranges, which are the blue- and red-light ranges.[30] The light from a white LED comprises three main ranges of light wavelength: blue (400–500 nm), green (450–600 nm), and red (550–750 nm) wavelengths, which fully cover two of the light wavelengths that Ce6 can absorb.[31,32] For these reasons, white LED surpassed red LED in the activation of Ce6, which resulted in a more effective eradication of Colon-26 cells and B16F10 melanoma cells.

The effect of DOX concentration on B16F10 melanoma cell viability was examined (Figure 3.5B), and it was discovered that a higher DOX concentration was associated with a reduction in B16F10 melanoma cell viability. Red and white LED irradiation were found to have no effect on the effectiveness of DOX in eradicating B16F10 melanoma cells when compared to no irradiation at all concentrations. This could be the same rationale for the previously mentioned usage of DOX to eradicate Colon-26 cells.

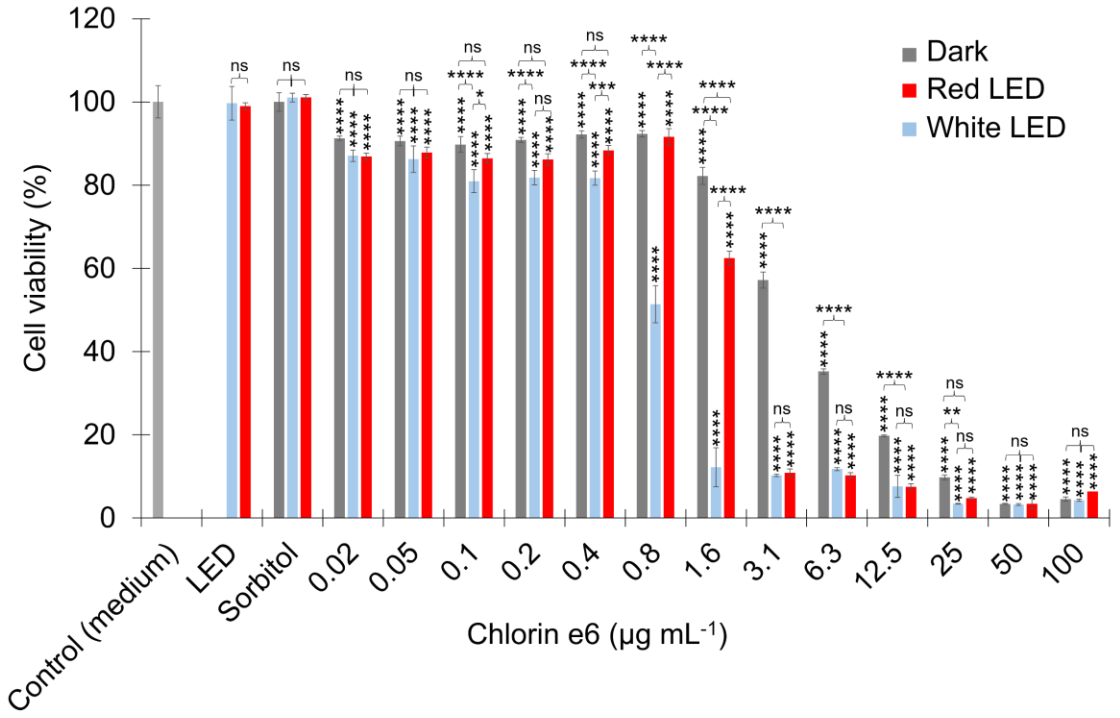
Dark
Red LED
White LED
Cell viability (%)
Chlorin e6 (µg mL-1)
Control (medium)
LED
Sorbitol
0.02
0.05
0.1
0.2
0.4
0.8
1.6
3.1
6.3
12.5
25
50
100

(A)

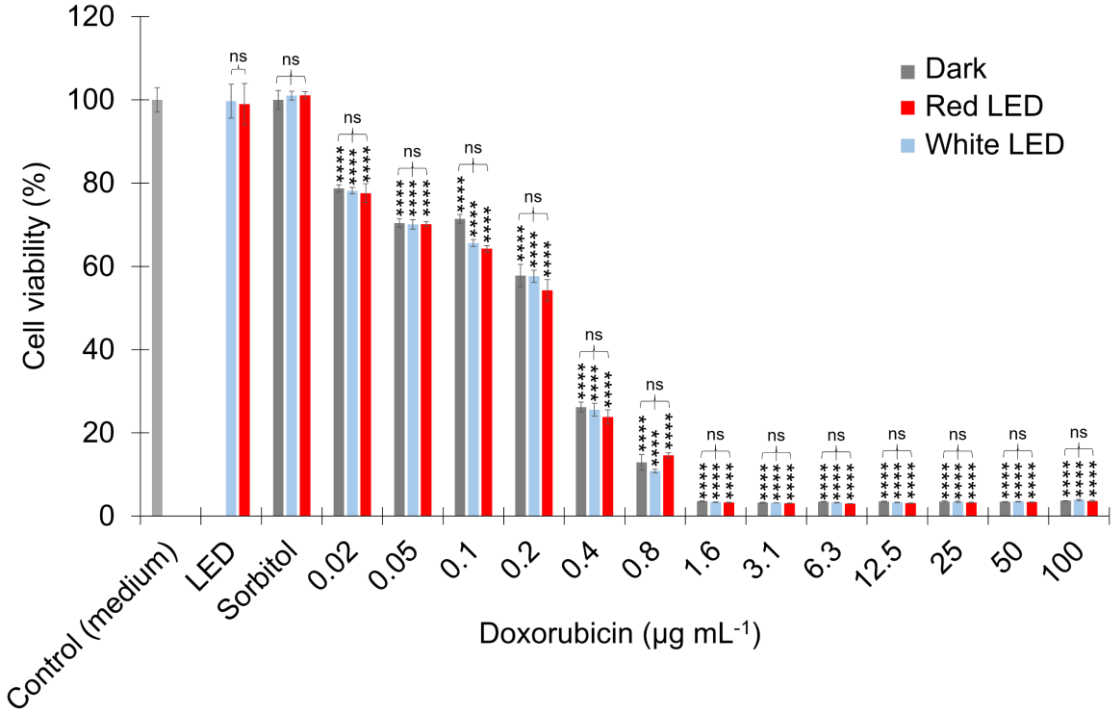
Dark
Red LED
White LED
Cell viability (%)
Doxorubicin (µg mL-1)
Control (medium)
LED
Sorbitol
0.02
0.05
0.1
0.2
0.4
0.8
1.6
3.1
6.3
12.5
25
50
100

(B)

Figure 3.5 *In vitro* viability of B16F10 melanoma cells treated with A) Ce6 and B) DOX (under dark, red LED shining, and white LED shining) including red LED, white LED, and sorbitol (5 mg mL^{-1}). Data are expressed as means ± standard error of the mean (SEM) (n = 5). Statistical analysis was assessed using one-way ANOVA followed by Tukey's test; ****, $p < 0.0001$; ***, $p < 0.001$; **, $p < 0.01$; *, $p < 0.05$.

3.5.3 The combination of Ce6 and DOX on Colon-26 cell viability under white LED shining

White LED is more efficient than red LED in activating Ce6 to generate ROS to eradicate both Colon-26 cells and B16F10 melanoma cells. In this part, we study the use of white LED with a combination of Ce6 and DOX on cell viability, comparing in the absence of light.

Considering the combination of Ce6 and DOX on Colon-26 cell viability, employing Ce6 in combination with DOX in various ratios under either dark or white LED conditions, as shown in figure 3.6. Under the dark condition, the efficiency of Colon-26 cell eradication employing the combination of Ce6 and DOX is lower than using DOX alone. Under the condition of white LED irradiation, it was found that the combination of Ce6 and DOX led to a higher efficiency of Colon-26 cell eradication than the use of either compound alone at the same concentration. The effectiveness of Ce6 and DOX when combined to eradicate cancer cells was investigated by examining the ratios of Ce6 to DOX at various ratios. The results showed that a ratio of Ce6 greater than DOX provided superior efficacy in eradicating Colon-26 cells (cell viability = 3.44% at Ce6: DOX of 8: 1). This ratio provided the efficiency of eradicating Colon-26 cells, which was better than both the ratio of Ce6 equal to DOX (cell viability = 3.63% at Ce6: DOX of 1: 1) and the ratio of DOX greater than Ce6 (cell viability = 12.28% at Ce6: DOX of 1: 8). The experimental results indicate that combining Ce6 with DOX and white LED irradiation provides a synergistic effect

that enhances the efficacy of Colon-26 cell eradication when compared to the use of either drug individually. The synergistic effect in eradicating Colon-26 cells was better when the ratio of Ce6 was greater than DOX.

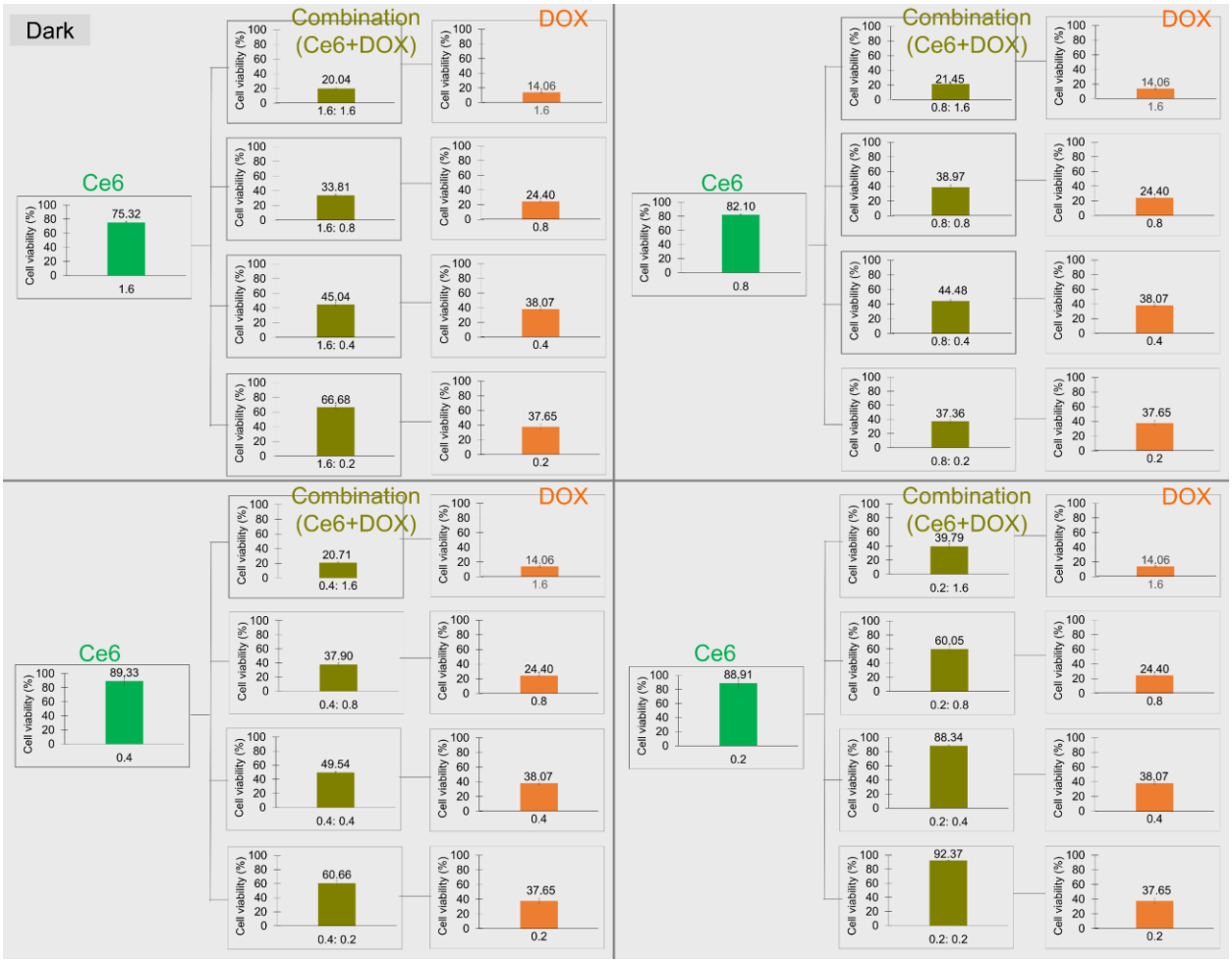

(A)

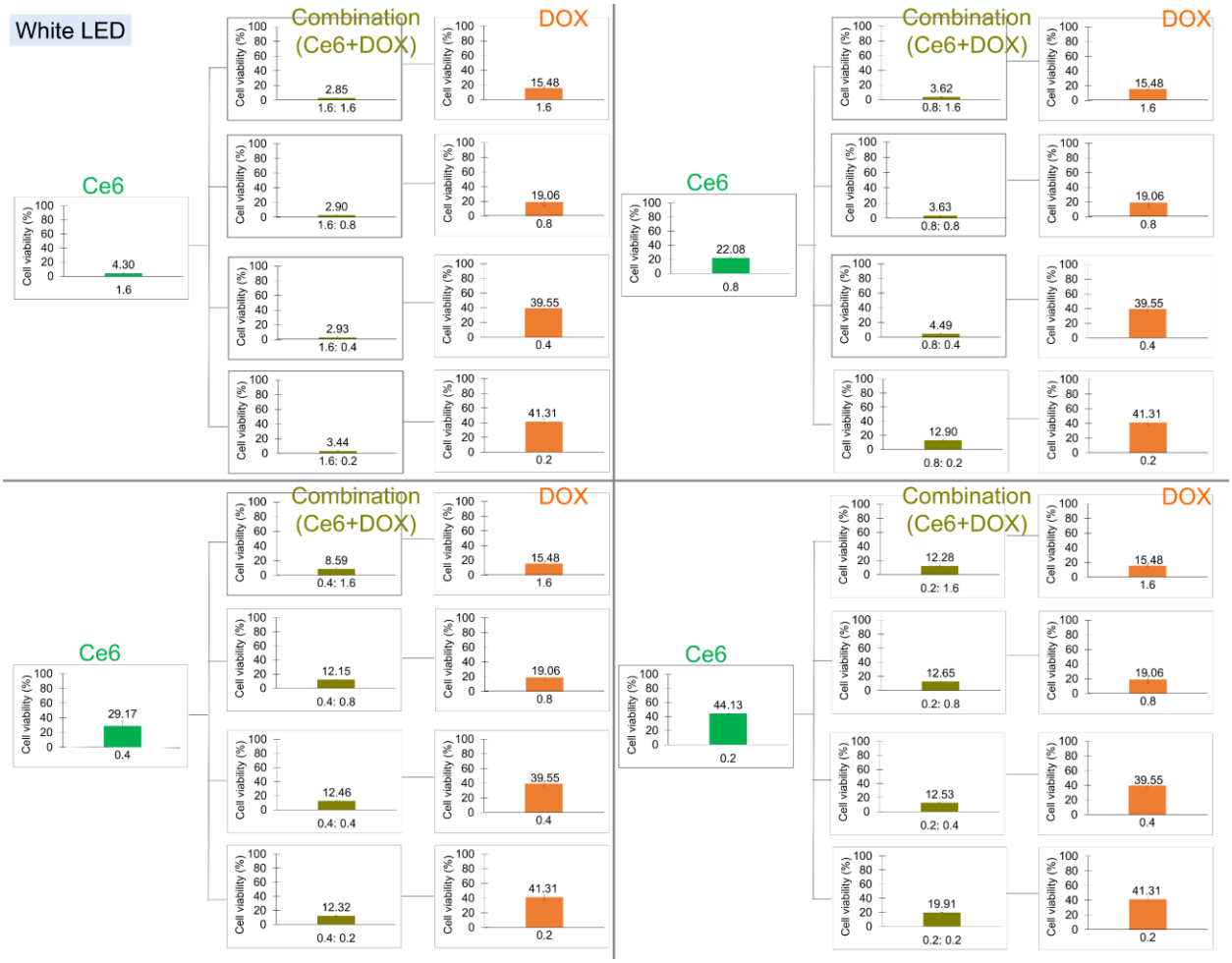

(B)

Figure 3.6 Viability of Colon-26 cells treated with Ce6, DOX, and the combination of Ce6 and DOX under the dark condition (A) and white LED irradiation (B) at various drug concentrations. Data are expressed as means ± standard error of the mean (SEM) (n = 5).

3.5.4 The combination of Ce6 and DOX on B16F10 melanoma cell viability

Ce6 in combination with DOX in various ratios under either dark or white LED conditions, as shown in figure 3.7. Under the dark condition, it was found that using Ce6 in combination with DOX at all concentrations did not result in improved eradication efficiency of B16F10 melanoma cells. The eradication efficiency of B16F10 melanoma cells is also lower than using

only DOX. Under the condition of white LED irradiation, it was found that the combination of Ce6 and DOX led to a higher eradication efficiency of B16F10 melanoma cells than the use of either compound alone at the same concentration. The effectiveness of Ce6 and DOX when combined to eradicate cancer cells was investigated by examining the ratios of Ce6 to DOX at various ratios. The results showed that a ratio of DOX greater than Ce6 provided superior efficacy in eradicating B16F10 melanoma cells (cell viability = 2.92% at DOX: Ce6 of 8: 1). This ratio provided the efficiency of eradicating B16F10 melanoma, which was better than both the ratio of Ce6 equal to DOX (cell viability = 4.26% at Ce6: DOX of 1: 1) and the ratio of Ce6 greater than DOX (cell viability = 10.84% at Ce6: DOX of 8: 1). The experimental results indicate that combining Ce6 with DOX and white LED irradiation provides a synergistic effect that enhances the efficacy of B16F10 melanoma cell eradication when compared to the use of either drug individually. The synergistic effect in eradicating B16F10 melanoma was better when the ratio of DOX was greater than Ce6.

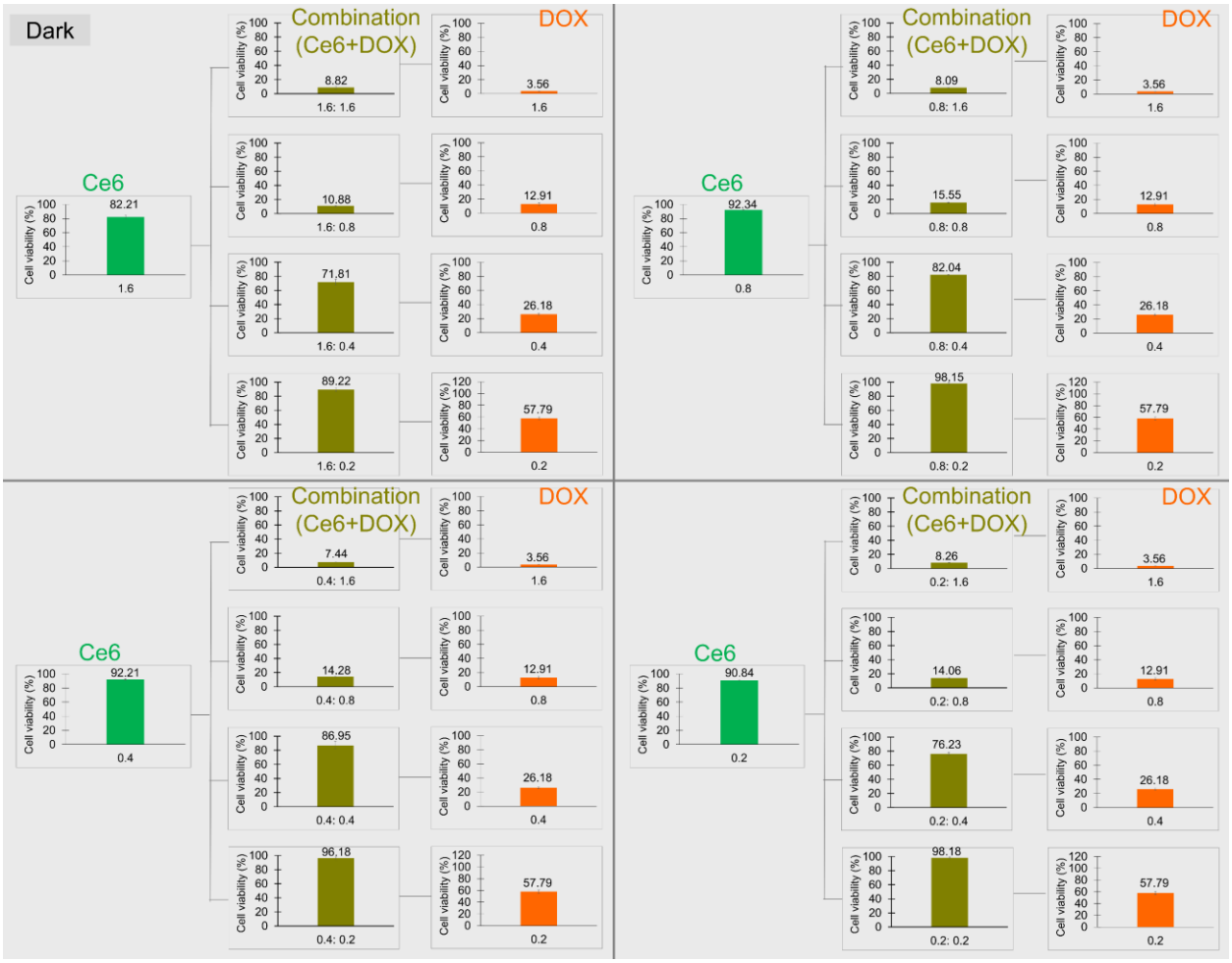
Dark
Ce6
Combination (Ce6+DOX)
DOX
Cell viability (%)
82.21
1.6
8.82
1.6: 1.6
3.56
1.6
10.88
1.6: 0.8
12.91
0.8
71.81
1.6: 0.4
26.18
0.4
89.22
1.6: 0.2
57.79
0.2
92.34
0.8
8.09
0.8: 1.6
15.55
0.8: 0.8
82.04
0.8: 0.4
98.15
0.8: 0.2
92.21
0.4
7.44
0.4: 1.6
14.28
0.4: 0.8
86.95
0.4: 0.4
96.18
0.4: 0.2
90.84
0.2
8.26
0.2: 1.6
14.06
0.2: 0.8
76.23
0.2: 0.4
98.18
0.2: 0.2

(A)

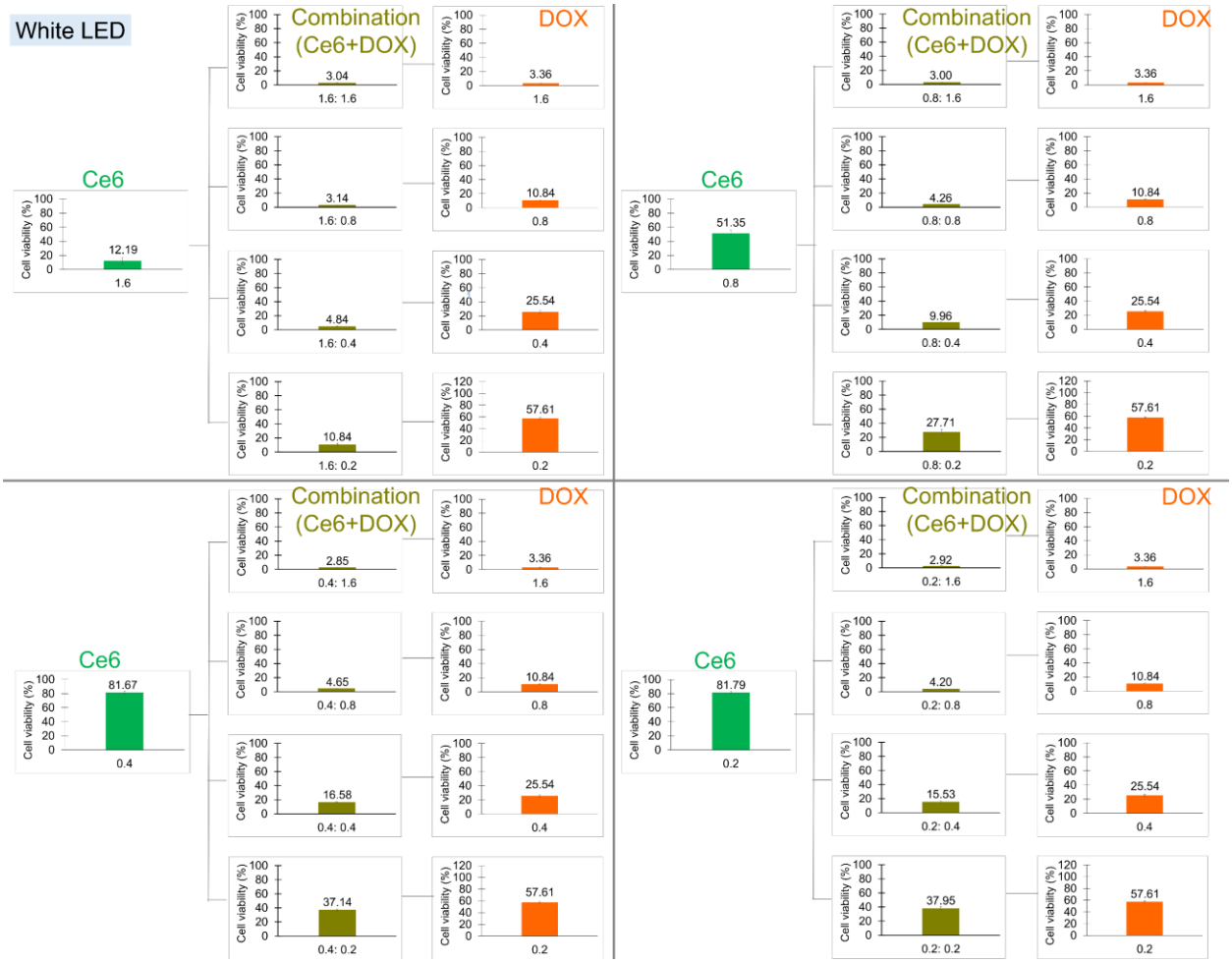

(B)

Figure 3.7 Viability of B16F10 melanoma cells treated with Ce6, DOX, and the combination of Ce6 and DOX under the dark condition (A) and white LED irradiation (B) at various drug concentrations. Data are expressed as means ± standard error of the mean (SEM) (n = 5).

3.6 Conclusion

Ce6 (a photosensitizer) and DOX (a chemotherapeutic drug) can eradicate both Colon-26 cells and B16F10 melanoma cells in cellular experiments. In the case of employing Ce6, the results demonstrated that both red LED and white LED irradiation could activate Ce6 to produce ROS in eradicating both Colon-26 cells and B16F10 melanoma cells more effectively than no irradiation.

Furthermore, a comparison between red and white LEDs revealed that white LED was noticeably more efficient than red LED at activating Ce6 to generate ROS, which eradicated Colon-26 cells and B16F10 melanoma cells more effectively. In the case of employing DOX, the results demonstrated that the use of red LED or white LED in DOX did not affect the effectiveness of the drug in eradicating both Colon-26 cells and B16F10 melanoma cells.

The following study investigated the efficacy of employing Ce6 and DOX combinations to eradicate Colon-26 cells and B16F10 melanoma cells in the presence of white LED light compared to the absence of light. The results demonstrated that a combination of Ce6 and DOX did not remove Colon-26 or B16F10 melanoma more effectively in dark conditions. The effectiveness of eradicating both Colon-26 cells and B16F10 melanoma cells was lower than using DOX alone. In contrast, the combination drugs under white LED irradiation provided a synergistic effect that surpasses the use of either treatment alone at the same concentration in terms of eradicating Colon-26 cells or B16F10 melanoma cells. Colon-26 cells were eradicated more efficiently when the ratio of Ce6 was greater than DOX in a combination. Meanwhile, B16F10 melanoma cells were eradicated more efficiently when the ratio of DOX was greater than Ce6 in a combination.

3.7 References

(1) Bonetto, A.; Rupert, J. E.; Barreto, R.; Zimmers, T. A. The Colon-26 Carcinoma Tumor-Bearing Mouse as a Model for the Study of Cancer Cachexia. *J. Vis. Exp.* **2016**, No. 117.

(2) *Colon-26*. Accegen.com. https://www.accegen.com/product/colon-26-abc-tc0154/ (accessed 2024-04-30).

(3) Tatebayashi, D.; Himori, K.; Yamada, R.; Ashida, Y.; Miyazaki, M.; Yamada, T. High-Intensity Eccentric Training Ameliorates Muscle Wasting in Colon 26 Tumor-Bearing Mice. *PLoS One* **2018**, *13* (6), e0199050.

(4) Masumoto, K.; Yamada, I.; Tanaka, H.; Fujise, Y.; Hashimoto, K. Tissue Distribution of a New Photosensitizer ATX-S10Na(II) and Effect of a Diode Laser (670 Nm) in Photodynamic Therapy. *Lasers Med. Sci.* **2003**, *18* (3), 134–138.

(5) Ogawara, K.-I.; Higaki, K. Nanoparticle-Based Photodynamic Therapy: Current Status and Future Application to Improve Outcomes of Cancer Treatment. *Chem. Pharm. Bull. (Tokyo)* **2017**, *65* (7), 637–641.

(6) Demeckova, V.; Mudronova, D.; Gancarcikova, S.; Kubatka, P.; Kajo, K.; Kassayova, M.; Bojkova, B.; Adamkov, M.; Solár, P. 5-Fluorouracil Treatment of CT26 Colon Cancer Is Compromised by Combined Therapy with IMMODIN. *Int. J. Mol. Sci.* **2022**, *23* (12), 6374.

(7) Taniura, T.; Iida, Y.; Kotani, H.; Ishitobi, K.; Tajima, Y.; Harada, M. Immunogenic Chemotherapy in Two Mouse Colon Cancer Models. *Cancer Sci.* **2020**, *111* (10), 3527–3539.

(8) Couto, G. K.; Segatto, N. V.; Oliveira, T. L.; Seixas, F. K.; Schachtschneider, K. M.; Collares, T. The Melding of Drug Screening Platforms for Melanoma. *Front. Oncol.* **2019**, *9*.

(9) Potez, M.; Trappetti, V.; Bouchet, A.; Fernandez-Palomo, C.; Güç, E.; Kilarski, W. W.; Hlushchuk, R.; Laissue, J.; Djonov, V. Characterization of a B16-F10 Melanoma Model Locally Implanted into the Ear Pinnae of C57BL/6 Mice. *PLoS One* **2018**, *13* (11), e0206693.

(10) Behera, S. P.; Tyagi, W.; Saxena, R. K. Carboxyl Nanodiamonds Inhibit Melanoma Tumor Metastases by Blocking Cellular Motility and Invasiveness. *PNAS Nexus* **2023**, *2* (11).

(11) Castano, A. P.; Demidova, T. N.; Hamblin, M. R. Mechanisms in Photodynamic Therapy: Part One—Photosensitizers, Photochemistry and Cellular Localization. *Photodiagnosis Photodyn. Ther.* **2004**, *1* (4), 279–293.

(12) Clement, S.; Sobhan, M.; Deng, W.; Camilleri, E.; Goldys, E. M. Nanoparticle-Mediated Singlet Oxygen Generation from Photosensitizers. *J. Photochem. Photobiol. A Chem.* **2017**, *332*, 66–71.

(13) Yoo, J.-O.; Ha, K.-S. New Insights into the Mechanisms for Photodynamic Therapy-Induced Cancer Cell Death. In *International Review of Cell and Molecular Biology*; Elsevier, **2012**; pp 139–174.

(14) Penjweini, R.; Deville, S.; Ethirajan, A.; Ameloot, M. Investigating the Intracellular Dynamics of Hypericin-Loaded Nanoparticles and Polyvinylpyrrolidone-Hypericin by Image Correlation Spectroscopy. In *Nanoscience in Dermatology*; Elsevier, **2016**; pp 275–286.

(15) Zhou, Z.; Song, J.; Nie, L.; Chen, X. Reactive Oxygen Species Generating Systems Meeting Challenges of Photodynamic Cancer Therapy. *Chem. Soc. Rev.* **2016**, *45* (23), 6597–6626.

(16) Yuan, B.; Wang, H.; Xu, J.-F.; Zhang, X. Activatable Photosensitizer for Smart Photodynamic Therapy Triggered by Reactive Oxygen Species in Tumor Cells. *ACS Appl. Mater. Interfaces* **2020**, *12* (24), 26982–26990.

(17) Baskaran, R.; Lee, J.; Yang, S.-G. Clinical Development of Photodynamic Agents and Therapeutic Applications. *Biomater. Res.* **2018**, *22* (1).

(18) García-Sánchez, M.; Rojas-González, F.; Menchaca-Campos, E.; Tello-Solís, S.; Quiroz-Segoviano, R.; Diaz-Alejo, L.; Salas-Bañales, E.; Campero, A. Crossed and Linked Histories of Tetrapyrrolic Macrocycles and Their Use for Engineering Pores within Sol-Gel Matrices. *Molecules* **2013**, *18* (1), 588–653.

(19) Belikov, A. V.; Kozlova, A. D.; Smirnov, S. N.; Fyodorova, Y. V. Investigation of the Changes in Extinction Spectrum of Modern Chlorine-Containing Photosensitizing Drugs under the Visible Light Action. *J. Biomed. Photonics Eng.* **2022**, *8* (4), 040502.

(20) Tampa, M.; Sarbu, M.-I.; Matei, C.; Mitran, C.-I.; Mitran, M.-I.; Caruntu, C.; Constantin, C.; Neagu, M.; Georgescu, S.-R. Photodynamic Therapy: A Hot Topic in Dermato-Oncology (Review). *Oncol. Lett.* **2019**.

(21) *Photodynamic therapy to treat cancer*. Cancer.gov. https://www.cancer.gov/about-cancer/treatment/types/photodynamic-therapy (accessed 2024-04-30).

(22) *Chlorin E6 - blog*. (n.d.). Glpbio.com. https://www.glpbio.com/blog/post/chlorin-e6.html (accessed 2024-11-14).

(23) Anand, U.; Dey, A.; Chandel, A. K. S.; Sanyal, R.; Mishra, A.; Pandey, D. K.; De Falco, V.; Upadhyay, A.; Kandimalla, R.; Chaudhary, A.; Dhanjal, J. K.; Dewanjee, S.; Vallamkondu, J.; Pérez de la Lastra, J. M. Cancer Chemotherapy and beyond: Current Status, Drug Candidates, Associated Risks and Progress in Targeted Therapeutics. *Genes Dis.* **2023**, *10* (4), 1367–1401.

(24) Starobova, H.; Vetter, I. Pathophysiology of Chemotherapy-Induced Peripheral Neuropathy. *Front. Mol. Neurosci.* **2017**, *10*.

(25) Sun, Y.; Liu, Y.; Ma, X.; Hu, H. The Influence of Cell Cycle Regulation on Chemotherapy. *Int. J. Mol. Sci.* **2021**, *22* (13), 6923.

(26) Liu, C.; Chen, H.; Guo, S.; Liu, Q.; Chen, Z.; Huang, H.; Zhao, Q.; Li, L.; Cen, H.; Jiang, Z.; Luo, Q.; Chen, X.; Zhao, J.; Chen, W.; Yang, P. C.; Wang, L. Anti-Breast Cancer-Induced Cardiomyopathy: Mechanisms and Future Directions. *Biomed. Pharmacother.* **2023**, *166* (115373), 115373.

(27) Sadeghi-Aliabadi, H.; Minaiyan, M.; Dabestan, A. Cytotoxic Evaluation of Doxorubicin in Combination with Simvastatin against Human Cancer Cells. *Res. Pharm. Sci.* **2010**, *5* (2), 127–133.

(28) Macpherson, N.; Belch, A.; Taylor, M.; Sutherland, J.; Czaykowski, P.; Connors, J. Liposomal Encapsulated Doxorubicin (Caelyx) in the Treatment of Relapsed Aggressive Non-Hodgkin's Lymphoma: A Phase II Study. *Leuk. Lymphoma* **2006**, *47* (7), 1327–1332.

(29) Meredith, A.-M.; Dass, C. R. Increasing Role of the Cancer Chemotherapeutic Doxorubicin in Cellular Metabolism. *J. Pharm. Pharmacol*. **2016**, *68* (6), 729–741.

(30) Kulichenko, A.; Farrakhova, D. S.; Yakovlev, D. V.; Maklygina, Y. S.; Shiryaev, A. A.; Loschenov, V. B. Fluorescence Diagnostics and Photodynamic Therapy of Squamous Cell Carcinoma of the Lateral Surface of the Tongue Using the Photosensitizer Chlorin E6 by Spectroscopic Video Fluorescence Methods. *J. Phys. Conf. Ser.* **2021**, *2058* (1), 012021.

(31) *Fundamentals of Light-Emitting Diodes (LEDs)*. Fsu.edu. https://zeiss-campus.magnet.fsu.edu/print/lightsources/leds-print.html (accessed 2024-05-01).

(32) David, A.; Whitehead, L. A. LED-Based White Light. *C. R. Phys.* **2018**, *19* (3), 169–181.

CHAPTER 4

In vivo anticancer therapeutic efficacy of MOD

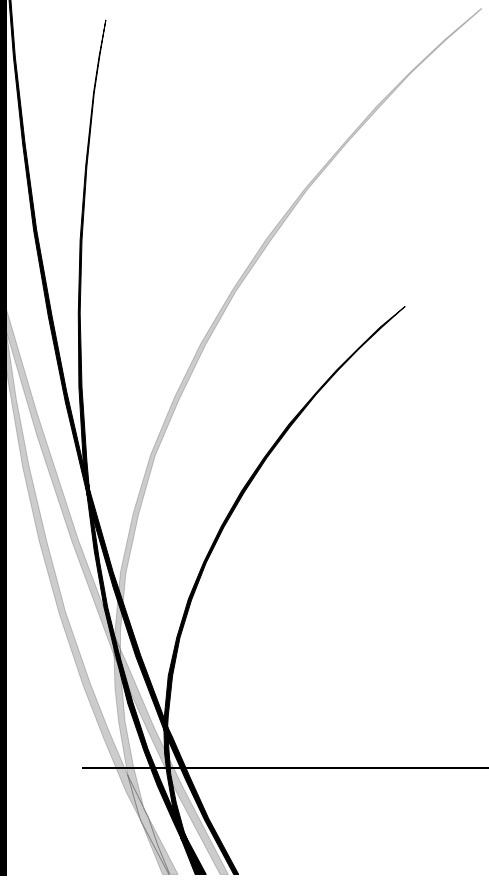

4.1 Introduction

Skin cancer, comprising various malignancies arising from the skin's epidermal and dermal layers, presents a significant public health concern globally. With rising incidence rates and diverse subtypes, effective management of skin cancer requires a nuanced approach that addresses tumor heterogeneity, treatment resistance, and individual patient characteristics.[1] In recent years, combination therapies have emerged as a promising strategy for enhancing treatment efficacy, minimizing toxicity, and improving outcomes in patients with skin cancer.[2,3] By integrating multiple treatment modalities, such as surgery, radiation therapy, chemotherapy, immunotherapy, and targeted therapy, combination treatments offer a multifaceted approach to combating this complex disease. Combination treatments for skin cancer encompass a diverse array of modalities, including surgery and radiation therapy, chemotherapy and immunotherapy, targeted therapy and immunotherapy, photodynamic therapy (PDT) and immunotherapy, and photodynamic therapy (PDT) and chemotherapy.[4-9] One of the combination treatments that is widely used to treat skin cancer is photodynamic therapy and chemotherapy. This combination offers several potential advantages for the treatment of skin cancer, including synergistic antitumor effects, the eradication of diverse tumor cell populations, minimizing the development of treatment resistance, and reducing treatment toxicity.[8-10] A number of studies have reported the use of photodynamic therapy in combination with chemotherapy for the treatment of skin cancer. For example, Chen et al.[8] investigated the use of two types of polymeric nanocarriers: 4-methylbenzyl alcohol-conjugated dextran (MA-DEX) and phenylboronic pinacol ester-conjugated dextran (PPE-Dex) to deliver chlorin e6 (Ce6, photosensitizer) and doxorubicin (DOX, a chemotherapeutic drug) and combined with 655 nm laser light to eradicate B16-F10 melanoma cells. The results demonstrated that employing Ce6 in combination with DOX and laser light had a synergistic effect that surpassed

the use of a single medication in the eradication of B16-F10 cells. Moreover, the materials used to create the polymeric nanocarriers also affect synergy in eradicating cancer cells. In all combinations of Ce6 and DOX, Dox-Ce6-loaded PPE-Dex was more effective than Dox-Ce6-loaded MA-Dex at eradicating B16-F10 cells because when Dox-Ce6-loaded PPE-Dex nanocarriers are irradiated with laser light, PPE-Dex nanocarriers can be triggered by the ROS generated, resulting in better drug release than MA-Dex nanocarriers, which are ROS-insensitive nanocarriers. In Fu et al.,[9] IR820 (photosensitizer) and cisplatin (chemotherapeutic drug) were delivered using dissolvable microneedles (DMNs) fabricated from vinylpyrrolidone—vinyl acetate copolymer (PVPVA) in the eradication of 4T1 mouse breast cancer cells. The results demonstrated that combining drugs with laser-shining reduces the size of the cancer tumor significantly more successfully than employing a single drug. Moreover, DMNs have a good degree of penetration into the skin and dissolve within 10 minutes.

Therefore, the objective of this research is to use chlorin e6 (Ce6, a photosensitizer) and doxorubicin (DOX, a chemotherapeutic drug) to eradicate Colon-26 tumor in Colon-26 tumor-bearing mice. The dissolvable microneedles (DMNs) fabricated from sorbitol (sorbitol-based DMNs) were employed to deliver both types of drugs into the Colon-26 tumor. Then, white light from a tiny LED is emitted to stimulate Ce6 activity and eradicate Colon-26 tumors in combination with DOX. The skin cancer treatment device that the researchers invented is called a microneedle optical device (MOD). It is anticipated that the MOD will advance in development and provide an optional avenue for the treatment of skin cancer.

4.2 Materials and methods

4.2.1 Preparation of gel containing chlorin e6 and doxorubicin (Ce6-DOX gel)

Ce6 (18 mg) was dissolved in ethanol (Nacalai Tesque Inc., Kyoto, Japan) (1 mL) while DOX (4.3 mg) was dissolved in distilled water (9 mL). The Ce6 and DOX solutions were then mixed. Then, xanthan gum (Tokyo Chemical Industry Co., Ltd., Tokyo, Japan) (30 mg) and Tween 80 (Sigma-Aldrich, St. Louis, MO, USA) (500 mg) were gently mixed with the solution, and then vigorously stirred until the solution became gel-like. Finally, the Ce6–DOX gel was kept overnight at 4°C to remove air bubbles. Prepared gels was warmed to 20°C before being used in experiments.

4.2.2 *In vivo* therapeutic effects of MOD

The animal experiments were approved by the Institutional Animal Care and Use Committee of JAIST and conducted at JAIST with the guidelines. To investigate *in vivo* anticancer therapy using Colon-26-bearing mice by injecting 100 μL of the culture medium/Matrigel (Dow Corning, Corning, NY, USA) mixture (v/v = 1:1) containing 1×10^6 cells into the left side of the backs of the nude mice (female; 6 weeks; n = 15; average weight = 18 g; BALB/cCrSIc-nu/nu; Japan SLC). After the tumor reached about 100 mm^3, the mice were separated into 6 groups of 5 mice per group: the first group that received no treatment, the second group received white-LED illumination alone, the third group that received topical application of Ce6–DOX gel (100 μL, containing 180 μg of Ce6 and 43 μg of DOX) without white LED shining, the fourth group that received DMNs containing Ce6 and DOX (Ce6–DOX-loaded DMNs, loaded with 180 μg of Ce6 and 43 μg of DOX) without white LED shining, the fifth group that received topical application of Ce6–DOX gel (100 μL, containing 180 μg of Ce6 and 43 μg of DOX) with white LED shining, and sixth group that received MOD (Ce6–DOX-loaded DMNs, loaded with 180 μg of Ce6 and 43 μg of DOX, with white LED shining). The application area was wiped with 70% ethanol and

allowed to dry before Ce6-DOX gel or Ce6–DOX-loaded DMNs were applied for 10 min equally. The support of the Ce6–DOX-loaded DMNs was then peeled off. After treating with Ce6–DOX gel or Ce6–DOX-loaded DMNs for 1 h, fourth and fifth group were irradiated with white LED all of time during the period of experiment. The body weight and tumor size were measured every other day for 18 days (Figure 4.1). The tumor volume was computed according to the equation[11]:

$$\text{Tumor volume } (\text{mm}^3) = \frac{\text{Length (mm) x Width}^2\ (\text{mm}^2)}{2}$$

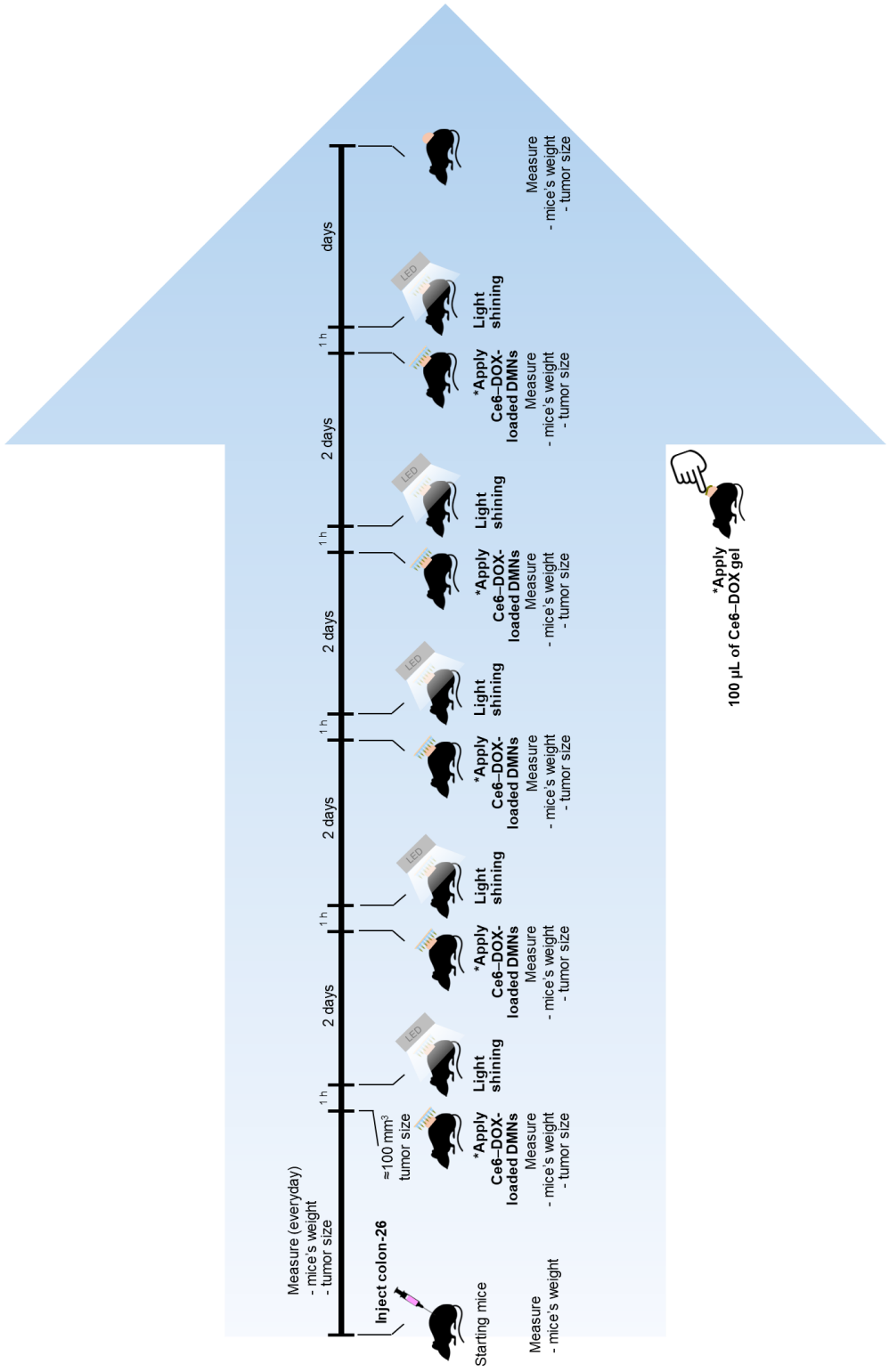

Figure 4.1 Timeline of photodynamic therapy using MOD.

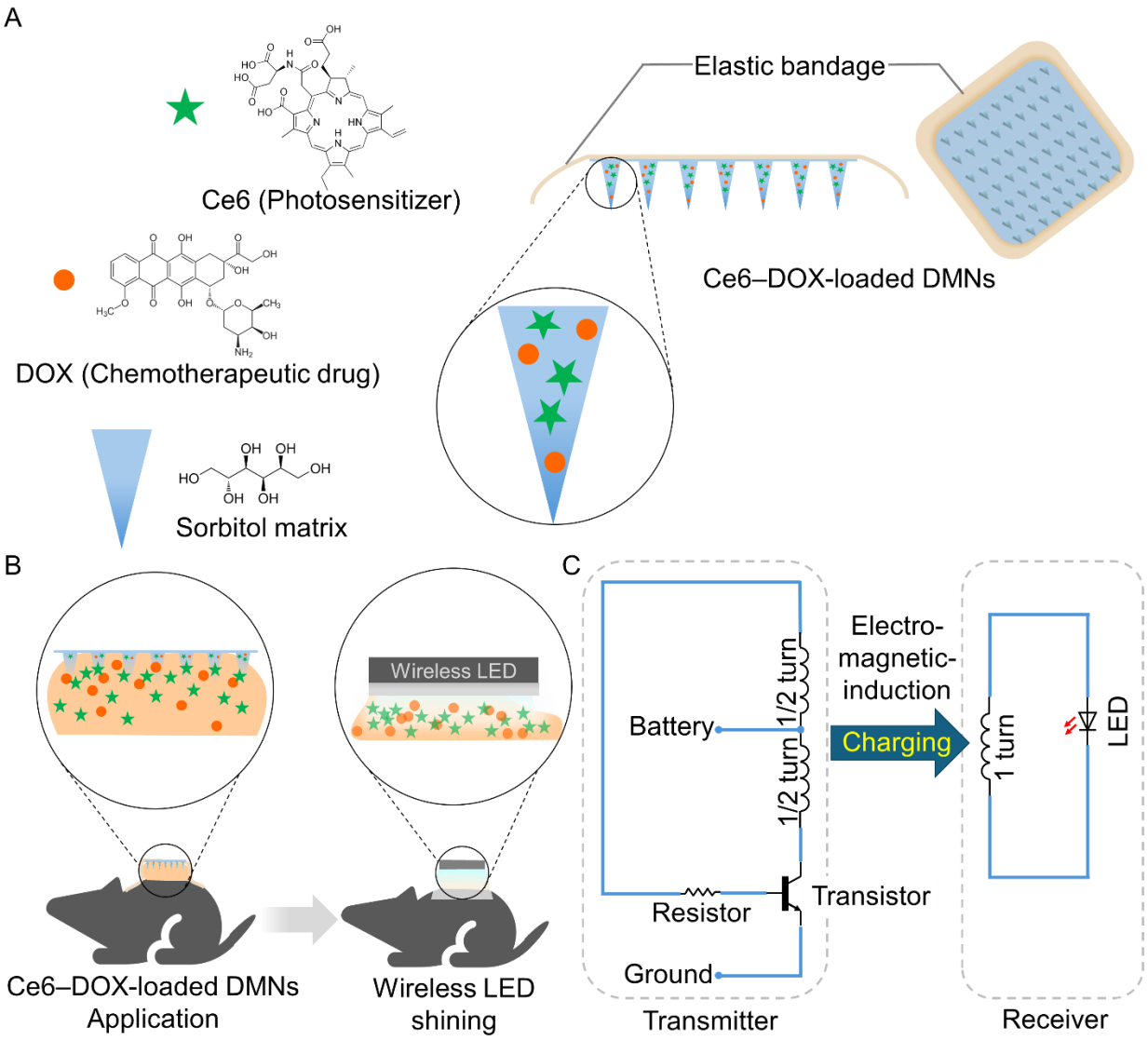

Figure 4.2 Schematic of the use of microneedle optical device (MOD) for treating skin cancer. A) The chemical composition and structure of Ce6–DOX-loaded dissolvable microneedles (DMNs). B) Two-step processes of using MOD for cancer cell eradication, which consists of applying Ce6–DOX-loaded DMNs and irradiating with the white LED. LEDs are wirelessly illuminated by a noncontact electro-charging system. C) Circuit diagrams for wireless charging of LED via electromagnetic induction.

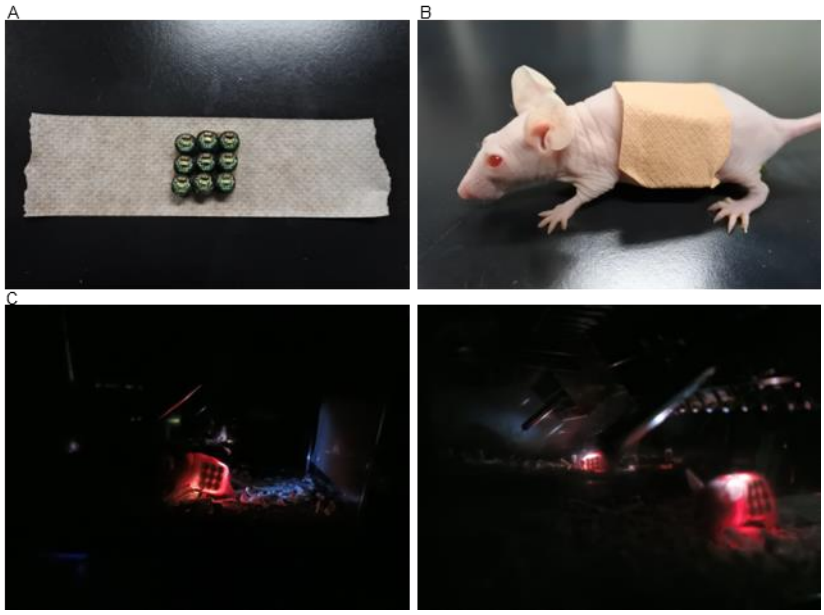

Figure 4.3 Photos of A) LEDs and a bandage, B) Colon-26 tumor-bearing mice with MOD, LEDs, and a bandage (before treatment), and C) optical treatment of Colon-26 tumor-bearing mice using the wireless LED light-driven MOD device.

4.2.3 Immunohistochemistry (IHC) staining of tumor tissues

The Colon-26 tumor-bearing mice were euthanized the day after the administration of Ce6–DOX gel or Ce6–DOX-loaded DMNs with white LED irradiation. The control groups did not receive any treatment. Thereafter, the tumor tissues from the different treatment groups were harvested for IHC staining. The IHC analysis was performed by Biopathology Institute Co., Ltd. (Oita, Japan) using standard protocols. Briefly, primary tumors were surgically removed, fixed in 10% formalin, processed for paraffin embedding, and cut into 3–4-μm-thick sections. After incubation with primary antibodies (listed in Table 4.1), the sections were stained with hematoxylin and examined using light microscopy (IX73)

Table 4.1 Antibodies used in this study.

Antibody	Type	Source	Catalog No.	Application
Caspase-3	Rabbit Polyclonal	Cell Signaling Technology	9661S	IHC (1: 100)
Anti-digoxigenin-peroxidase	Sheep Polyclonal	Merck Millipore	S7100	Tunel

4.3 Results and discussions

4.3.1 *In vivo* therapeutic effects of MOD

The efficacy of treating Colon-26 tumor-bearing mice was investigated by comparing the use of Ce6–DOX gel and Ce6–DOX-loaded DMNs with equivalent doses of each drug with/without shining a white LED to activate Ce6's activity to work with DOX in the treatment of Colon-26 tumors. Colon-26 tumor-bearing mice were treated every other day, and the tumor size and mice's weight were recorded throughout the experiment (Figure 4.4 A, D). The results demonstrated that without any treatment (control) and treating with white LED alone, the size of the tumor grew rapidly. At the end of the experiment, the tumor without any treatment (control) or treating with white LED alone was 15.3 times or 10.3 times larger than it had been on day 8. Meanwhile, the Ce6–DOX gel treatment or Ce6–DOX DMNs treatment without shining white LED displayed a partial tumor inhibitory effect; the tumor continued to grow and become larger, but it grew at a slower rate than the control. At the end of the experiment, the tumor treated with Ce6–DOX gel or Ce6–DOX DMNs was 8.6 times or 7.2 times larger than the day of the first treatment (day 8).

When the white LED was applied, Ce6–DOX gel or Ce6–DOX DMNs demonstrated against tumor growth better than Ce6–DOX gel or Ce6–DOX DMNs without white LED shining. Comparing Ce6–DOX gel with white LED shining and Ce6–DOX DMNs with white LED shining (MOD), the results demonstrated that MOD can inhibit tumor growth better than Ce6–DOX gel with white LED. At the end of the experiment, the tumor treated with MOD was only 3.4 times larger compared to the day of the first treatment. Meanwhile, the tumor treated with Ce6–DOX gel with white LED was 5.6 times larger compared to the day of the first treatment (day 8) (Figure 4.4 B, C). The experiment in this part reveals that the drug delivery method is as crucial as the drug's efficacy. Even though the drug has the same dosage and efficacy, different delivery methods result in different treatment efficacy. Apart from suggesting that drug delivery via DMNs is more efficient than topical application, photodynamic therapy can effectively treat cancer through the use of white LED.

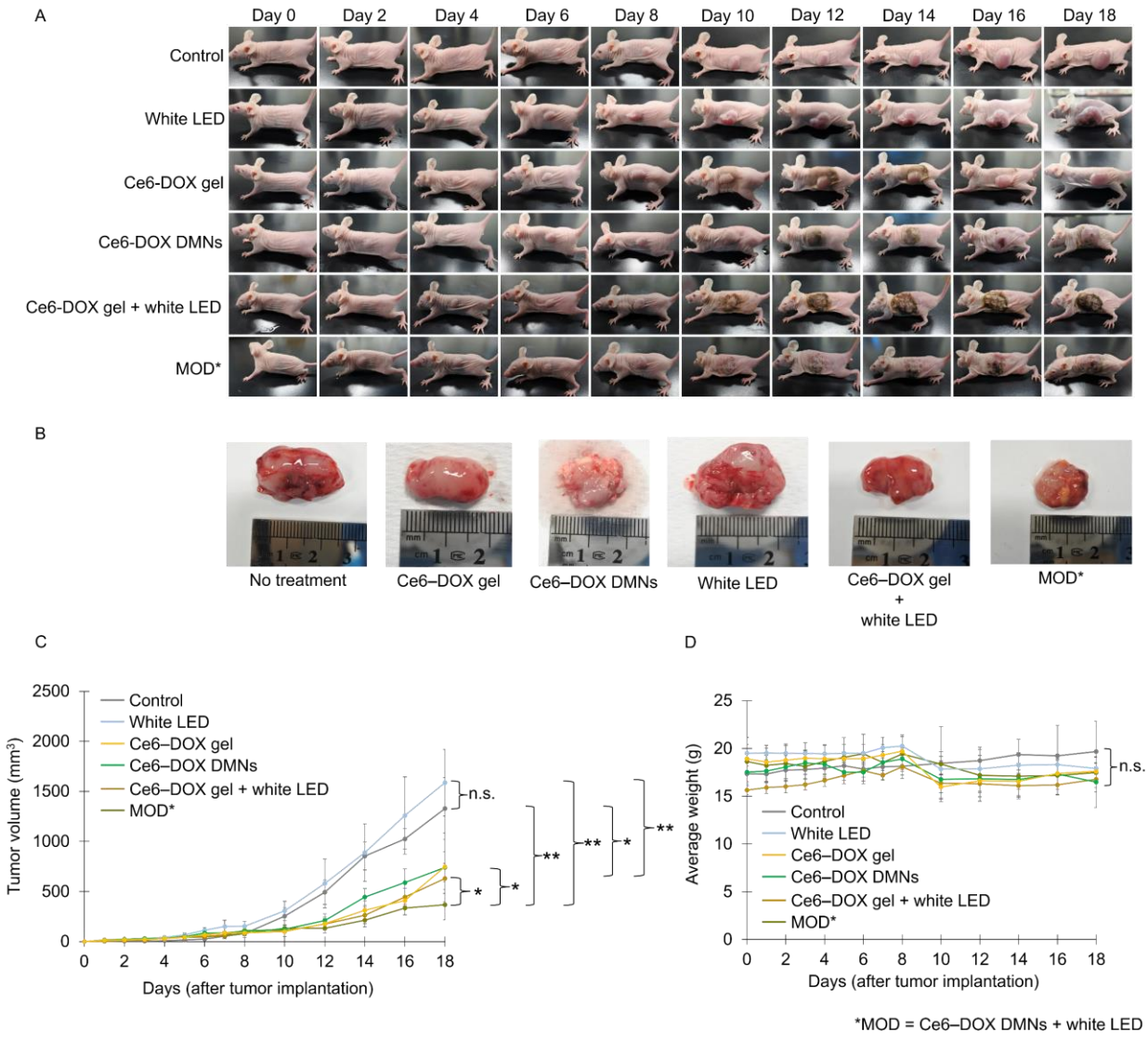

Figure 4.4 *In vivo* therapeutic efficacies of Ce6–DOX gel and Ce6–DOX-loaded DMNs against Colon-26 tumor-bearing BALB/c-nu/nu mice. A) Images of Colon-26 tumor-bearing mice with no treatment (negative control), white LED alone, Ce6–DOX gel with/without white LED irradiation, and Ce6–DOX-loaded DMN with/without white LED irradiation groups. B) Photos of excised tumors at the end of each treatment (Day 18). C) Tumor growth profiles with each treatment. Data are expressed as means ± standard error of the mean (SEM) (n = 5 biologically independent tests). Significance was assessed using one-way ANOVA followed by Tukey's test;

**, $p < 0.01$ and *, $p < 0.05$. D) Body weight of mice throughout the animal experiment. Data are expressed as means ± standard error of the mean (SEM) (n = 5 biologically independent tests). Significance was assessed using one-way ANOVA followed by Tukey's test; n.s., not significant.

Figure 4.5 Photos of the mouse after attachment of Ce6–DOX-loaded DMNs. Ce6–DOX-loaded DMNs were completely dissolved into skin after application just for 10 min.

4.3.2 Immunohistochemistry (IHC) staining of tumor tissues

In order to investigate whether the use of Ce6–DOX gel or Ce6–DOX-loaded DMNs with/without white LED shining affects the effectiveness of Colon-26 cell eradication, the tumor tissues from Colon-26 tumor-bearing mice after the first treatment were isolated and stained for histological analysis. Cellular apoptosis in tumors was examined using terminal deoxynucleotidyl transferase–mediated 2′-deoxyuridine, 5′-triphosphate nick end labeling (TUNEL) and cleaved-caspase 3 staining, and the pattern, shape, and structure of cells in a tumor were examined via hematoxylin and eosin (H&E) staining. The experimental results (Figure 4.6) demonstrate that cell apoptosis was almost rarely observed in the control, Ce6–DOX gel without white LED shining, and Ce6–

DOX-loaded DMNs without white LED shining. Histological analysis of tumor is no obvious change were found. Meanwhile, treating cancer via Ce6–DOX gel with white LED shining and MOD (Ce6–DOX-loaded DMNs with white LED shining) has been found to be effective in inhibiting cancer cells by inducing a higher level of cell apoptosis than other groups (Figure 4.7). However, when Ce6–DOX gel with white LED shining and MOD were compared, it was discovered that MOD caused a greater degree of cell apoptosis than Ce6–DOX gel with white LED shining. A significant region of severe cellular destruction was discovered in the Colon-26 tumor-bearing mice receiving MOD. According to these results, white LEDs are effective enough to be developed for photodynamic therapy. When combined with DMN devices, their efficacy surpasses that of topical application and enhances the efficacy of cancer treatment.

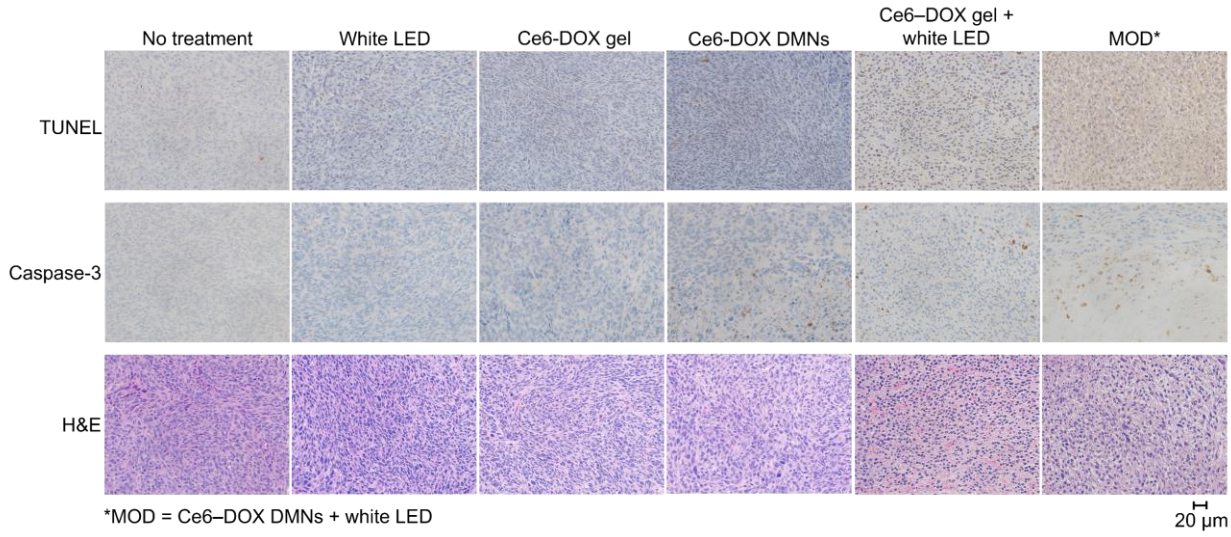

Figure 4.6 Histological analysis (TUNEL, caspase-3, and H&E staining) of tumor tissues after treatment with control (no treatment), white LED, Ce6–DOX gel, Ce6–DOX-loaded DMNs, Ce6–DOX gel with white LED and MOD (Ce6–DOX-loaded DMNs with white LED).

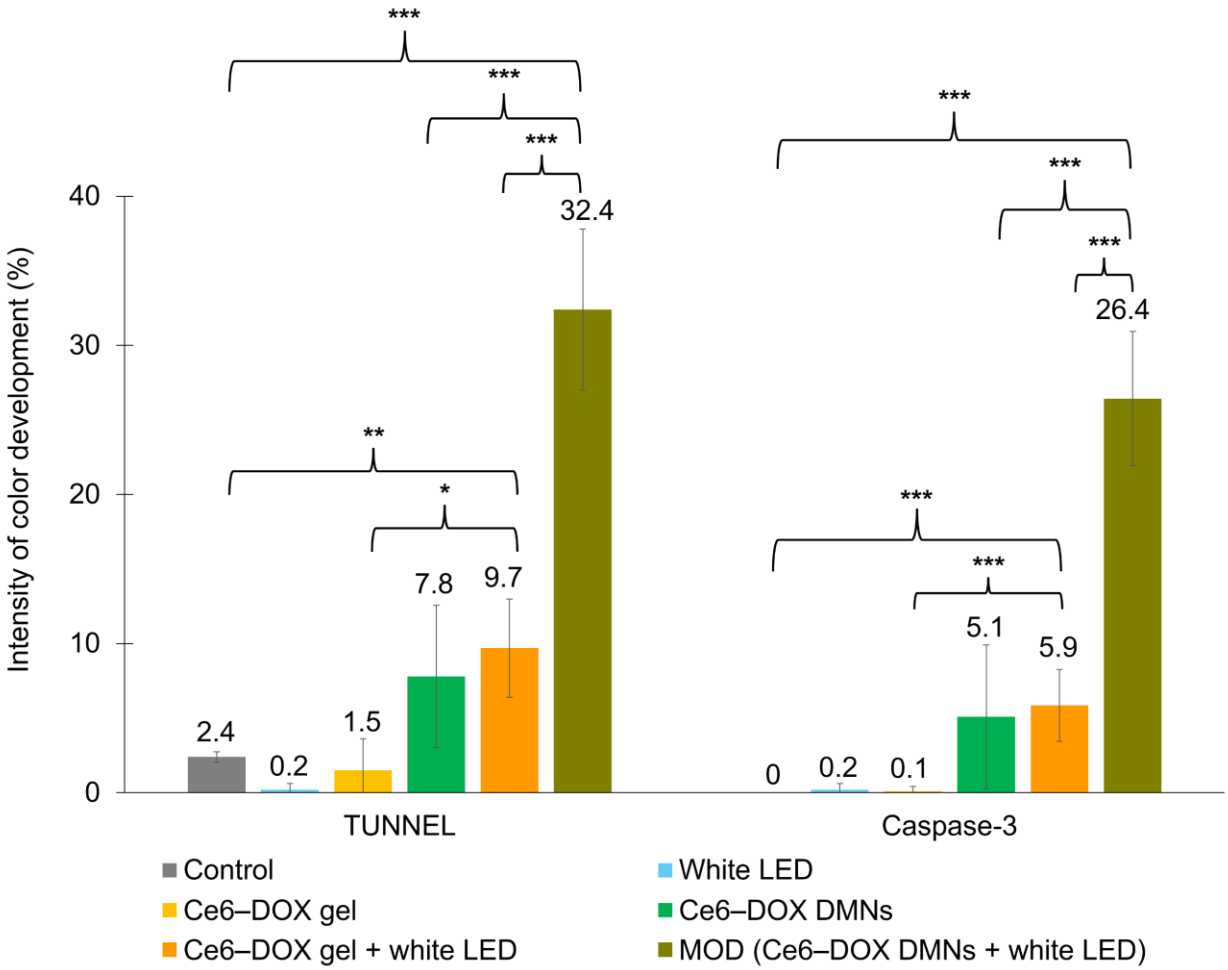

Figure 4.7 Intensity of color development (TUNEL and caspase-3) of tumor tissues after treatment with control (no treatment), white LED, Ce6–DOX gel, Ce6–DOX-loaded DMNs, Ce6–DOX gel with white LED and MOD (Ce6–DOX-loaded DMNs with white LED). Significance was assessed using one-way ANOVA followed by Tukey's test; ***, $p < 0.001$; **, $p < 0.01$ and *, $p < 0.05$.

4.4 Conclusion

MOD was successful in inhibiting the growth of the Colon-26 tumor. However, Ce6–DOX-loaded DMNs, a component of MOD, without white LED did not show effectiveness against tumor growth. Consequently, it can be argued that white LED plays a crucial role in activating Ce6 to

generate ROS in combination with DOX to eradicate the Colon-26 tumor. When white LEDs were employed with Ce6–DOX-loaded DMNs or Ce6–DOX gel, the results demonstrated that Ce6–DOX-loaded DMNs with white LED shining (MOD) provide the effectiveness against tumor growth better than Ce6–DOX gel with white LED shining. These results demonstrated that the effectiveness of DMNs for drug delivery surpasses that of topical application and improves the effectiveness of cancer treatment as well, under white LED shining. In histological analysis results, the Colon-26 tumor treated with MOD exhibited the highest level of cell apoptosis compared to other groups. A significant region of severe cellular destruction was discovered in the Colon-26 tumor-bearing mice receiving MOD. With the success of using MOD in treating skin cancer, the researcher consequently anticipates that MOD will be evolved into a self-used device for skin cancer treatment.

4.5 References

(1) Azimi, A.; Fernandez-Peñas, P. Molecular Classifiers in Skin Cancers: Challenges and Promises. *Cancers (Basel)* **2023**, *15* (18), 4463.

(2) Mokhtari, R. B.; Homayouni, T. S.; Baluch, N.; Morgatskaya, E.; Kumar, S.; Das, B.; Yeger, H. Combination Therapy in Combating Cancer. *Oncotarget* **2017**, *8* (23), 38022–38043.

(3) Rager, T.; Eckburg, A.; Patel, M.; Qiu, R.; Gantiwala, S.; Dovalovsky, K.; Fan, K.; Lam, K.; Roesler, C.; Rastogi, A.; Gautam, S.; Dube, N.; Morgan, B.; Nasifuzzaman, S. M.; Ramaswami, D.; Gnanasekar, V.; Smith, J.; Merchant, A.; Puri, N. Treatment of Metastatic Melanoma with a Combination of Immunotherapies and Molecularly Targeted Therapies. *Cancers (Basel)* **2022**, *14* (15), 3779.

(4) Hortobagyi, G. N.; Ames, F. C.; Buzdar, A. U.; Kau, S. W.; McNeese, M. D.; Paulus, D.; Hug, V.; Holmes, F. A.; Romsdahl, M. M.; Fraschini, G.; McBride, C. M.; Martin, R. G.; Montague, E. Management of Stage III Primary Breast Cancer with Primary Chemotherapy, Surgery, and Radiation Therapy. *Cancer* **1988**, *62* (12), 2507–2516.

(5) Sordo-Bahamonde, C.; Lorenzo-Herrero, S.; Gonzalez-Rodriguez, A. P.; Martínez-Pérez, A.; Rodrigo, J. P.; García-Pedrero, J. M.; Gonzalez, S. Chemo-Immunotherapy: A New Trend in Cancer Treatment. *Cancers (Basel)* **2023**, *15* (11), 2912.

(6) Wargo, J. A.; Cooper, Z. A.; Flaherty, K. T. Universes Collide: Combining Immunotherapy with Targeted Therapy for Cancer. *Cancer Discov.* **2014**, *4* (12), 1377–1386.

(7) Zha, M.; Yang, G.; Li, Y.; Zhang, C.; Li, B.; Li, K. Recent Advances in AIEgen-based Photodynamic Therapy and Immunotherapy. *Adv. Healthc. Mater.* **2021**, *10* (24).

(8) Chen, Y.; Gao, Y.; Li, Y.; Wang, K.; Zhu, J. Synergistic Chemo-Photodynamic Therapy Mediated by Light-Activated ROS-Degradable Nanocarriers. *J. Mater. Chem. B Mater. Biol. Med.* **2019**, *7* (3), 460–468.

(9) Fu, J.-J.; Li, C.-W.; Liu, Y.; Chen, M.-Y.; Zhang, Q.; Yu, X.-Y.; Wu, B.; Li, J.-X.; Du, L.-R.; Dang, Y.-Y.; Wu, D.; Wei, M.-Y.; Lin, Z.-Q.; Lei, X.-P. The Microneedles Carrying Cisplatin and IR820 to Perform Synergistic Chemo-Photodynamic Therapy against Breast Cancer. *J. Nanobiotechnology* **2020**, *18* (1).

(10) Rajan, S. S.; Chandran, R.; Abrahamse, H. Overcoming Challenges in Cancer Treatment: Nano-enabled Photodynamic Therapy as a Viable Solution. *Wiley Interdiscip. Rev. Nanomed. Nanobiotechnol.* **2024**, *16* (1).

(11) Sápi, J.; Kovács, L.; Drexler, D. A.; Kocsis, P.; Gajári, D.; Sápi, Z. Tumor Volume Estimation and Quasi-Continuous Administration for Most Effective Bevacizumab Therapy. *PLoS One* **2015**, *10* (11), e0142190.

CHAPTER 5

General conclusion

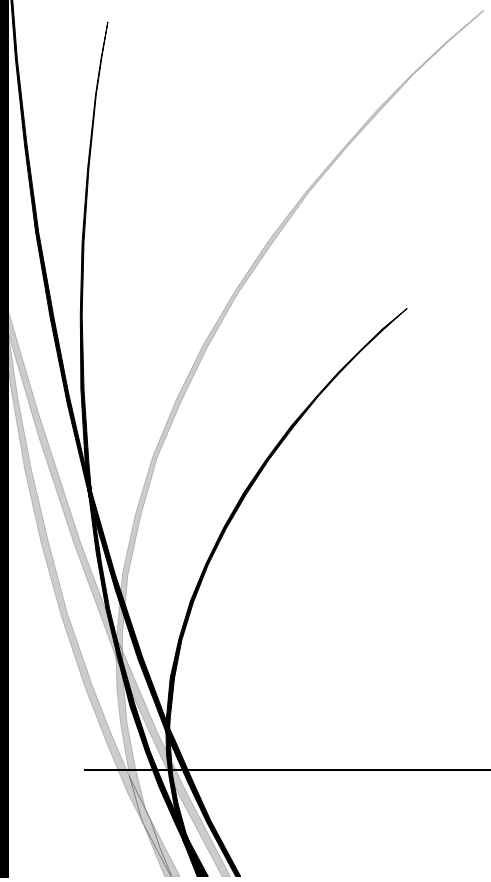

General conclusion

DMNs with an array of 13x12 needles and an average needle height of 1000 μm were successfully created through the simple micromolding method. DMNs have strong enough needles to penetrate skin, which delivers the model drug into the skin and allows enhanced drug distribution over topical treatments (*ex vivo* and *in vitro*). The efficacy of drugs (Ce6 and DOX) combining with LEDs (red and white LEDs) in eradicating model cancer cells (Colon-26 cells and B16F16 melanoma cells) was also investigated. The results demonstrated that combining Ce6 and DOX along with an irradiating white LED provided a synergistic effect, resulting in the highest efficiency in eradicating both Colon-26 cells and B16F10 melanoma cells.

Following the results of previous experiments, we developed the microneedle optical device (MOD), which consists of Ce6–DOX-loaded DMNs and white LED. When MOD was applied to study the inhibition of the Colon-26 tumor in mice, the results demonstrated that applying MOD provided significantly greater tumor growth inhibition in terms of enhanced cell apoptosis and cell membrane destruction than Ce6–DOX-loaded DMNs alone, Ce6–DOX gel with/without white LED, and control (no treatment). At the end of the experiment, Colon-26 tumor-bearing mice that received MOD treatment had tumors that were noticeably smaller than those of Colon-26 tumor-bearing mice that received other treatments. Regarding the efficacy of MOD in treating Colon-26 tumor-bearing mice, the researchers expect that MOD will be further evolved into a self-use device for skin cancer patients, following the dermatologist's instructions.

Acknowledgments

I have been incredibly supported and assisted while I worked on this dissertation.

First of all, I would like to sincerely thank Prof. Eijiro MIYAKO for welcoming me into his lab and for providing me with an awesome platform that allowed me to gain knowledge and relevant experimental skills in the field of cell culture and animal experiment. I would like to sincerely thank Prof. Kazuaki MATSUMURA, who role as my second supervisor and supported me to complete this dissertation. I would like to acknowledge Prof. Supason WANICHWECHARUNGRUANG, whose continued guidance and support really taught me a lot in microneedle experiments as well as living. I would also like to express my thanks to all the members of the MIYAKO laboratory who have helped me in my research with their important advice and support.

I would like to thank Prof. Motoichi KURISAWA for supporting and assisting me to complete my minor research project.

My deepest gratitude goes out to the JAIST-Chulalongkorn University dual degree program for supporting both my scholarship and my living expenses in Japan.

Finally, I want to express my gratitude to my friends and family for their understanding advice and empathetic ear.